KEYNOTE ARTICLE

Molecular Recognition among Alcohols and Amines: Super-tetrahedral Crystal Architectures of Linear Diphenol–Diamine Complexes and Aminophenols

Otto Ermer* and Andreas Eling
Institut für Organische Chemie der Universität, Greinstrasse 4, D-50939 Köln, Germany

Hydroxy and amino groups are complementary as regards hydrogen-bond donors and acceptors. This is expected to lead to molecular recognition among alcohols and primary amines, *i.e.*, to a propensity towards formation of 1:1 alcohol–amine complexes, driven by a 50% increase of the number of hydrogen bonds as compared with the uncomplexed constituents. Possible hydrogen-bonded architectures of such complexes are suggested, and the concept is successfully exploited for crystal engineering purposes by drawing upon linear diphenols, aromatic diamines, and amino-phenols as supramolecular partners. Specifically, the crystal-structural chemistry is reported of the 1:1 molecular complexes between hydroquinone and *p*-phenylenediamine, hydroquinone and benzidine, 4,4′-dihydroxybiphenyl and *p*-phenylenediamine, 4,4′-dihydroxybiphenyl and benzidine, as well as of *p*-aminophenol, and of 4,4′-hydroxyaminobiphenyl. The diphenol–diamine complexes form hydrogen-bonded super-diamond lattices with 1.5 O(H)N bonds per oxygen and nitrogen atoms, respectively. Again exclusively *via* O(H)N bonds, the aminophenol structures are also super-tetrahedral but after the manner of the polar wurtzite variant. Some similar reported structures are analysed in the light of the present concepts and results, and implications are discussed of the finding that molecular recognition is possible among molecules as standard as simple alcohols and amines.

Introduction

Alcohols and primary amines molecules do not completely satisfy, by themselves, their valencies for hydrogen bonding. This follows simply from the fact that the number of the respective donors and acceptors is different. While the hydroxy function can donate one H atom to a hydrogen bond and possesses two oxygen lone pairs as acceptors, the amino group involves two donor H atoms but only one acceptor lone pair (Fig. 1). Therefore, crystalline alcohols and primary amines can form only one hydrogen bond per hydroxy and amino group, respectively, and necessarily have to dispense with a potentially possible, additional half hydrogen bond per OH and NH_2 group, respectively. Usually, crystalline alcohols and amines build up hydrogen-bonded (zig-zag or helical) chains with one 'silent' hydroxy lone pair and amino hydrogen atom, respectively (Fig. 2). However, cyclic patterns are also known, especially among polyfunctional alcohols, well-known examples being pentaerythritol[1] with hydrogen-bonded $(OH)_4$ rings and hydroquinone[2] with $(OH)_6$ rings. Thus, two hydrogen bonds emanate from each oxygen and nitrogen atom, respectively, in the chain, *i.e.*, one counts one hydrogen bond per oxygen and nitrogen atom, respectively.

With regard to hydrogen bonding, alcohols and amines are obviously complementary both stoichiometrically and geometrically. Interchange of H-bond donors and acceptors transforms the bonding pattern of the hydroxy group into that of the amino group, and *vice versa*, and in both cases the geometrical disposition of valencies is tetrahedral (Fig. 1). Therefore, molecular recognition[3] may be expected between alcohols and primary amines since complementarity represents the crucial prerequisite supporting favourable interactions between the molecular partners. In a 1:1 alcohol–amine complex the number of H-bond donors and acceptors is balanced and the possibility opens up for complete saturation of all potential H-bond valencies. Within fourfold tetrahedral coordination, from every oxygen and nitrogen atom three hydrogen bonds would then emanate, as compared with only two in the free alcohol and amine, respectively. Per O and N atom one would then count 1.5 hydrogen bonds in the 'super-tetrahedral' 1:1 alcohol–amine complex, the formation of which is thus seen to be accompanied by a 50% increase in the number of H bonds.

Fig. 1 H-Bond donor–acceptor complementarity of alcohols and amines

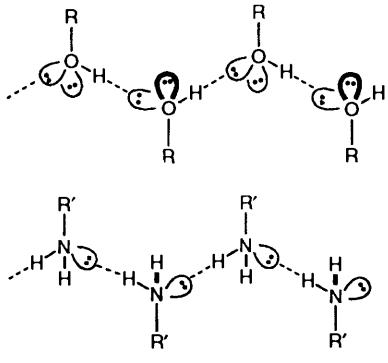

Fig. 2 Usual chain-like pattern of H-bonding in alcohols (top) and amines (bottom) with one H-bond per O and N atoms, respectively

It is worth noting in the present context that the water molecule is self-complementary as regards optimal hydrogen bonding since, of course, it involves two donors (H atoms) and two acceptors (lone pairs) with tetrahedral directionality (Fig. 3). In crystalline water, therefore, the two maximally possible hydrogen bonds per oxygen atom may be made by building up

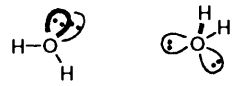

Fig. 3 Donor–acceptor self-complementarity of water

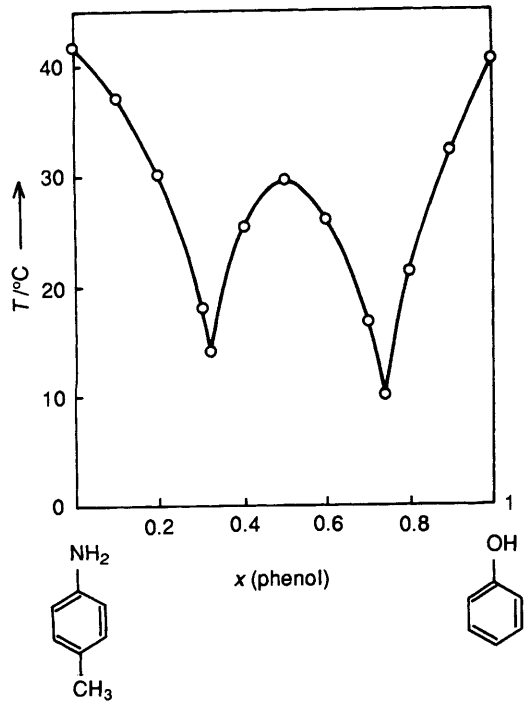

Fig. 4 Melting-point diagram of the binary system phenol–*p*-toluidine (adapted from ref. 6)

a super-tetrahedral three-dimensional framework with four hydrogen bonds emanating from each oxygen atom. The normal hexagonal polymorph of ice (ice-I_h) has a super-wurtzite (hexagonal diamond, tridymite) architecture, the slightly less stable cubic form (ice-I_c) a super-diamond (cristobalite) structure, and a cubic high-pressure form (ice-VII, VIII) is double-diamondoid with two interpenetrating super-diamond networks; other high-pressure polymorphs of ice also have super-tetrahedral structures, albeit distorted.[4a] However, despite the complete saturation of H-bond valencies, water is not fully satisfied either, since the O(H)O hydrogen bonds cannot attain lengths short enough to prevent porous super-tetrahedral frameworks of ice-I_h and I_c.[4b] The energetic disadvantage of this hollowness of the normal ice structure contributes to give rise to a variety of most important characteristic and unique water properties, such as the density anomaly of ice-water, propensity of hydrate and clathrate formation, extremely versatile hydration, solvation, and catalytic properties.

The possible 50% increase of the number of hydrogen bonds stated above should clearly provide a significant driving force towards formation of 1:1 complexes between alcohols and primary amines. Support in favour of this conjecture may for instance be gleaned from a survey of melting-point diagrams[5] of binary alcohol–amine mixtures, which quite frequently show pronounced dystectic maxima (congruent melting points) at 1:1 hydroxy–amino stoichiometry indicating the expected 1:1 complex formation; as a typical example the melting point diagram of the system phenol–*p*-toluidine[6] is reproduced in Fig. 4. It is noted parenthetically that from simple melting-point diagrams quite generally valuable information may be derived as regards molecular recognition phenomena, *i.e.*, supramolecular complex formation. Unfortunately, comprehensive and up-to-date respective thermochemical tabulations of phase equilibria and melting diagrams are not readily available.

Various reasonable structural possibilities with maximum H-bonding may be foreseen for 1:1 complexes between alcohols, R–OH, and primary amines, R′–NH_2 (Figs. 5 and 6). The usual hydrogen-bonded alcohol and amine zig-zag chains of Fig. 2 may simply be joined together alternately by N(H)O hydrogen bonds [Fig. 5(*a*)] generating puckered sheets of *trans*-fused 'super-cyclohexane' rings with chair-like 'super-conformations'. These sheets are held together exclusively by hydrogen bonds, one third each of the type O(H)O, N(H)N and N(H)O. Topologically, they may be related to the sheet structure of the stable allotrope of (grey) arsenic and be referred to as 'super-arsenic' sheets, which in turn may be cut out of both the cubic diamond (zincblende, cristobalite) lattice and the hexagonal diamond (wurtzite, tridymite) lattice. From generation of the H-bonded super-arsenic sheets of Fig. 5(*a*) from the H-bonded alcohol and amine chains (Fig. 2) by means of N(H)O bonds, the 50% increase in the number of H bonds, *i.e.*, the new N(H)O bonds, becomes particularly obvious on complex formation. In the sheets we have 1.5 H bonds per O and N atom, respectively, as compared with only 1.0 in the chains of the constituent free alcohols and amines, respectively.

It appears reasonable to expect, in our complexes, a general tendency to avoid N(H)N hydrogen bonds, which, according to known structural evidence and electronegativity considerations are particularly weak, *i.e.*, comparatively long and of low polarity. N(H)N bonds may indeed be completely avoided if the hydrogen-bonded super-arsenic sheets are entirely made up of (stronger) N(H)O bonds, *i.e.*, if the alcohol and amine molecules are rearranged in such a way that each oxygen atom has exclusively nitrogen atoms as hydrogen-bonded neighbours, and each nitrogen atom exclusively oxygen neighbours [Fig. 5(*b*)]. Less regular or irregular (disordered) distributions of O(H)O, N(H)N and N(H)O bonds in the super-arsenic sheets are, in principle, also conceivable. Whatever the distribution, however, it is clear that the numbers of N(H)N and O(H)O bonds must always be equal, *i.e.*, transforming an N(H)O bond in Fig. 5(*b*) into an N(H)N bond is necessarily to be accompanied by transformation of another N(H)O bond into an O(H)O bond. It must be conceded, however, that this stoichiometric necessity appears to weaken the expected propensity of N(H)N avoidance since it is coupled to O(H)O avoidance of equal extent, and the latter type of hydrogen bond is of course relatively strong. The experimental results of our work reported further on nevertheless indicate complete N(H)O preference in the alcohol–amine complexes studied.

If two thirds of the *trans*-fusions between the super-cyclohexane chairs of Figs. 5(*a*), (*b*) are replaced by *cis*-fusions such as shown in Fig. 5(*c*), one arrives at H-bonded sheets analogous to those of black phosphorus, which again may be cut out of the cubic, yet not the hexagonal diamond lattice. Only the variant with N(H)O bonds throughout is drawn in Fig. 5(*c*). It would appear that the super-black phosphorus sheets of Fig. 5(*c*) are more restricted with regard to the size of the residues R and R′, respectively, than are the super-arsenic sheets of Fig. 5(*b*).

An intriguing structural possibility for 1:1 alcohol–amine complexes are polyhedral H-bonded architectures as depicted in Fig. 6. In principle, any polyhedron may be considered with three edges emanating from each vertex. (Polyhedra of this kind necessarily have the required even number of vertices since their number of edges is of course equal to 1.5 times the number of vertices.) In the following, we discuss a number of highly symmetric possibilities. Thus, polyhedral H-bond clusters taking the shape of a tetrahedron [Fig. 6(*a*)], a cube [Fig. 6(*b*)], or a pentagonal dodecahedron [Fig. 6(*c*)] may be envisaged. While the small tetrahedral cluster is angularly unfavourable with H-bonds heavily bent outward, and the large, angularly almost ideal dodecahedral cage is hollow requiring suitable

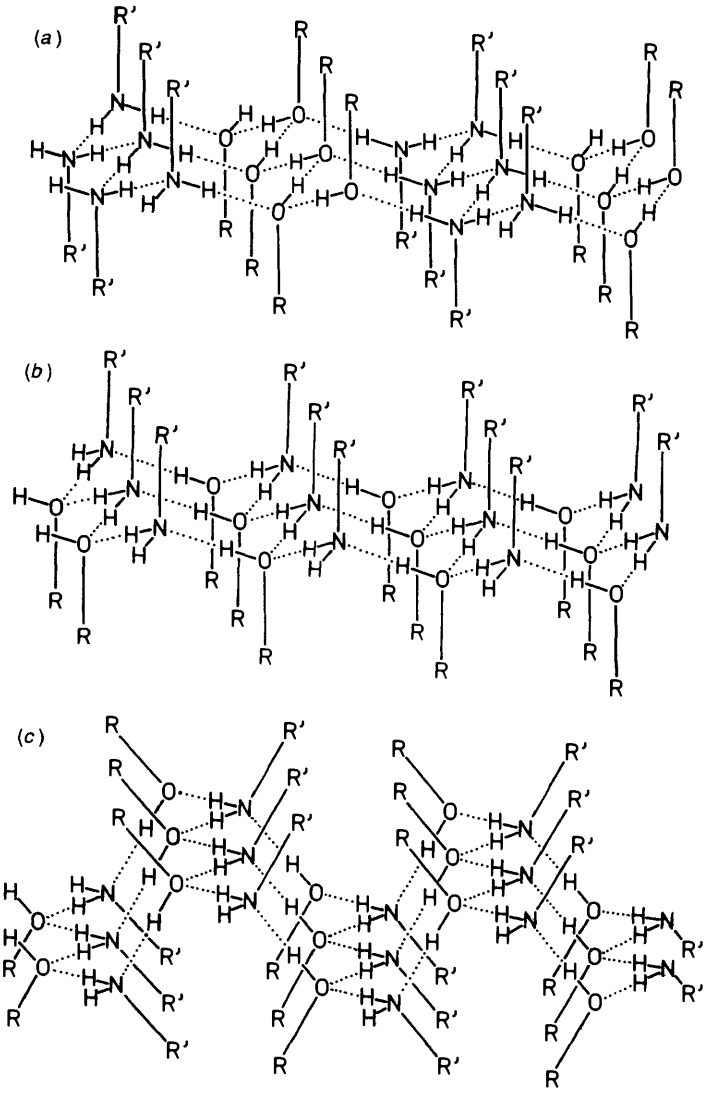

Fig. 5 H-Bonded sheets of a 1 : 1 alcohol–amine complex: (*a*) super-arsenic type with $\frac{1}{3}$ O(H)O, N(H)N and O(H)N bonds each; (*b*) super-arsenic type with O(H)N bonds exclusively; (*c*) super-black phosphorus type with O(H)N bonds exclusively

guest species for stabilization, the cube-shaped complex appears acceptable in both these respects. Interestingly, a cube-shaped octameric $(H_2O)_8$ cluster H-bonded analogously to Fig. 6(*b*) (four H-atoms not involved in cluster bonding) has recently been invoked in modelling the heat capacity of water.[7] Dodecahedral $(H_2O)_{20}$ clusters (10 H-atoms not involved in cluster bonding) play a prominent role as hosts in water clathrates.[8] Apart from the above Platonian polyhedra, for instance trigonal-prismatic, truncated-octahedral, or even extremely hollow truncated-icosahedral H-bonded clusters within 1 : 1 alcohol–amine complexes may be conceived [Figs. 6(*d*)–(*f*)]; inspiration for still other polyhedral possibilities may be gleaned from water clathrate studies.[8a] The huge truncated icosahedral cluster with 60 vertices (angularly somewhat unfavourable with H-bonds bent inward) has of course the topology of a modern soccer ball; its central cavity would indeed have about the right size to house an analogously shaped C_{60} (covalent) cluster! Similarly, a truncated-icosahedral H-bonded $(H_2O)_{60}$ cluster would provide a rather intriguing model for hydration of C_{60}; some of the 30 O–H bonds not involved in the cluster bonding could in fact point inward to form H bonds with the enclathrated C_{60} molecule similar to those in the water–benzene system.[9]

It is clear that in the envisaged polyhedral alcohol–amine complexes N(H)N [and O(H)O] bonds can only be completely avoided if all polygons (faces) of the underlying polyhedra have even numbers of vertices [Figs. 6(*b*), (*e*)], in which cases the H-bonding may be accomplished entirely by N(H)O bonds. Finally, it is noted that for simple topological reasons (see above) in the polyhedral complexes of Fig. 6 one of course again counts 1.5 hydrogen bonds per oxygen and nitrogen atom, respectively, as in the sheet-like architectures of Fig. 5. Thus polyhedral alcohol–amine complex formation again benefits from a 50% increase of the number of H-bonds, as compared with the uncomplexed educts.

In order to create genuinely favourable conditions for 1 : 1 alcohol–amine complex formation, *i.e.*, to improve the constituents' mutual molecular recognition, the sizes and shapes of the residues R and R′, and possibly also their specific intermolecular interactions have to be properly adjusted (tuned). Model considerations and density estimates, as well as the melting-point diagram of the binary system phenol–*p*-toluidine (see above, Fig. 4), and the crystal structure of *p*-aminophenol (see below) indicate that the phenyl group offers favourable prerequisites in support of H-bonded super-arsenic sheets as shown in Figs. 5(*a*), (*b*). Linear aliphatic side chains R, R′ also appear to fit reasonably well into an H-bond architecture of this kind. Bulkier substituents R, R′ than phenyl or ethyl are expected to favour the formation of small polyhedral alcohol–amine complexes [*e.g.*, the cases of Figs. 6(*a*), (*b*), (*d*)] with severely curved convex outer cluster surfaces, whereas smaller residues could provide a steric incentive to

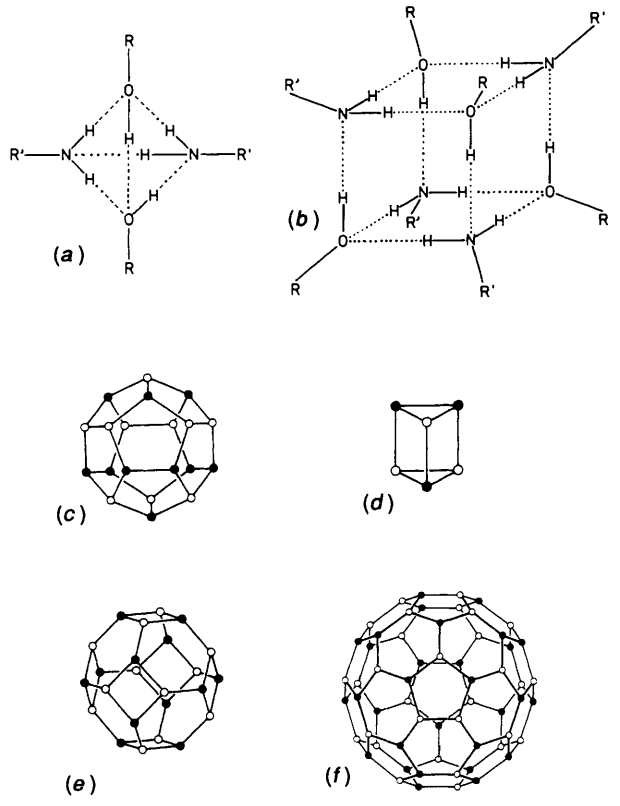

Fig. 6 Hypothetical polyhedral 1:1 alcohol–amine complexes. The H-bonded clusters take the shapes of a tetrahedron (*a*), cube (*b*), pentagonal dodecahedron (*c*), trigonal prism (*d*), truncated octahedron (*e*), truncated icosahedron (*f*). The possibilities (*a*) and (*b*) are shown in full, otherwise only oxygen and nitrogen atoms are drawn (empty and filled circles, respectively) and interconnected by straight lines representing the H-bonds.

build up larger polyhedral clusters [*e.g.*, as in Figs. 6(*c*), (*e*), (*f*)] with their smaller curvatures offering lesser convex space. For example, a tetrahedral 1:1 complex as sketched in Fig. 6(*a*) appears feasible between the bulky molecules of triphenylmethanol (trityl alcohol) and triphenylmethylamine (tritylamine); the crystal structure of trityl alcohol[10] is suggestive in this sense since it consists of tetrahedral tetramers similar to the envisaged complex structure.

Conceptually, the two-dimensional super-arsenic sheets of Figs. 5(*a*), (*b*) may be joined to build up three-dimensional super-tetrahedral, *i.e.*, in particular super-diamond or super-wurtzite, networks through replacing the monofunctional alcohol and amine components R–OH and R′–NH_2 by linear dialcohols HO–R_{di}–OH and diamines H_2N–R'_{di}–NH_2, respectively [Figs. 7(*a*), (*b*)]. We have recently been interested in H-bonded (multiple) super-diamond architectures of tetrahedral tetracarboxylic acids with intriguing properties, for example remarkable solid-state inclusion behaviour.[11] Suitable choices for R_{di} and R'_{di} appeared to be 1,4-phenylene and 4,4′-biphenylylene, and we report here the crystal structures of the possible 1:1 complexes between hydroquinone **1**, 4,4′-dihydroxybiphenyl **2**, *p*-phenylenediamine **3**, and benzidine **4**, *i.e.*, the molecular compounds **1·3**, **1·4**, **2·3** and **2·4**. The 'supramolecular synthesis'[12] of these adducts turned out to be straightforward as expected from our structural design outlined above, and likewise their crystal architectures comply with the anticipated super-tetrahedral properties, as shown in the following. Obviously, the selection of dialcohols and diamines for our complexation experiments also has crystallographic virtues since the 3-dimensional H-bonded networks represent relatively rigid molecular assemblies as compared with the sheet-like patterns expected in 1:1 complexes of monoalcohols

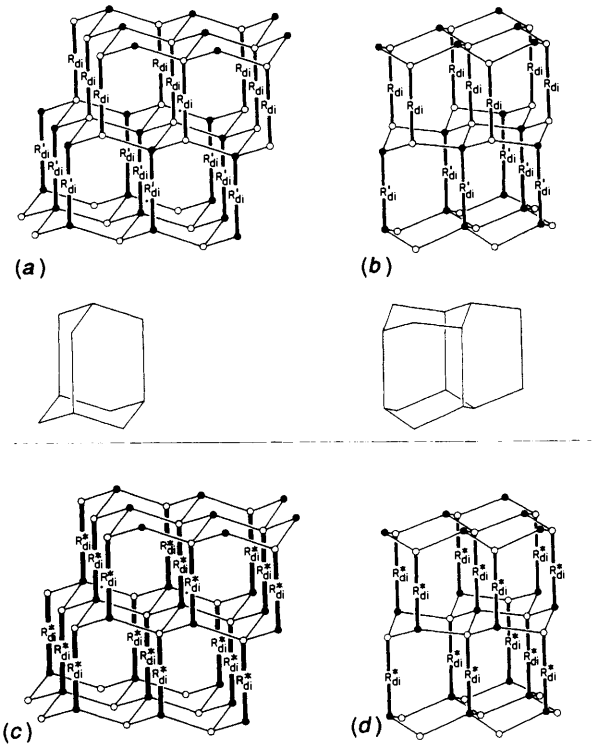

Fig. 7 3D super-tetrahedral H-bonded architectures of 1:1 complexes between linear dialcohols, HO–R_{di}–OH, and linear diamines, H_2N–R'_{di}–NH_2, and of linear amino alcohols, HO–R^*_{di}–NH_2. Oxygen atoms are represented as empty, nitrogen atoms as filled circles. The covalent linear linkers R_{di}, R'_{di} and R^*_{di} are drawn as thick rods, the H-bonds as thin lines omitting the bridging H atoms. The aggregation of the molecules is such that exclusively O(H)N hydrogen bonds are formed: (*a*) super-diamond network of dialcohol–diamine complex; super-adamantane building block diagrammatically shown below; (*b*) super-wurtzite network of dialcohol–diamine complex; combined super-iceane and super-bicyclo[2.2.2]octane building block below; (*c*) super-diamond, (*d*) super-wurtzite network of amino alcohol. The complexes **1·3**, **1·4**, **2·3** and **2·4** described in this paper aggregate diamond-like (*a*) in the crystal, the aminophenols **5** and **6** wurtzite-like (*d*).

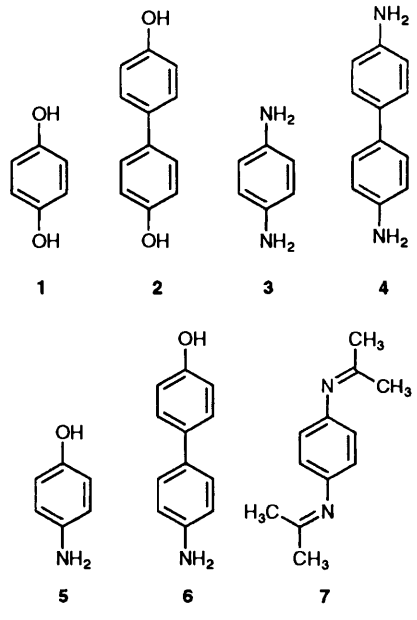

and monoamines. Furthermore, the complexes involving hydroquinone **1** could be expected to form with particular ease since **1** is well known to possess a pronounced propensity to engage in inclusion compounds and molecular complexes.[2,13]

Table 1 Crystallographic details of the X-ray measurements[a]

Molecular system	1·3	1·4	2·3	2·4	5	6
Crystal system	Monoclinic	Monoclinic	Monoclinic	Monoclinic	Orthorhombic	Orthorhombic
Space group	$P2_1/c$	$P2_1/c$	$P2_1/c$	$P2_1/c$	$Pna2_1$	$Pna2_1$
Z	2	2	2	2	4	4
a/Å	13.0889(12)	17.094(3)	17.397(3)	21.321(3)	8.184(1)	8.096(1)
b/Å	5.2291(8)	5.351(1)	5.345(1)	5.403(1)	5.262(1)	5.396(1)
c/Å	8.2427(8)	8.130(3)	8.111(2)	8.076(1)	12.951(2)	21.217(2)
β/°	98.714(8)	92.68(2)	101.05(2)	95.61(1)		
V/Å^3	557.6(1)	742.8(3)	740.2(3)	925.9(2)	557.7(2)	926.9(2)
d_x/g cm^{-3}	1.300	1.316	1.320	1.329	1.300	1.327
d_m/g cm^{-3}	—	—	1.31	1.34	1.30	1.32
θ_{max}/°	30	27	27	27	30	27
N_{tot}	2163	2213	2174	2724	1196	1293
N_{indep}	1627	1617	1610	2015	912	1037
$[F_o/\sigma(F_o)]_{min}$	4	4	4	4	4	3
N_{ref}	1386	927	1007	1476	728	668
N_{var}	101	136	136	171	101	171
ρ_{res}/e Å^{-3}	0.23	0.42	0.17	0.15	0.18	0.20
p	0.0001	0.04	0.0005	0.0001	0.04	0.0006
R	0.043	0.065	0.049	0.043	0.043	0.055
R_w	0.045	0.072	0.049	0.041	0.047	0.049

[a] Collection of intensities on a CAD4 4-circle diffractometer at room temperature; Mo Kα radiation with λ = 0.710 69 Å; reflection weights in the refinements $w(F_o) = [\sigma^2(F_o) + pF_o^2]^{-1}$; reflections with $F_o/\sigma(F_o) < [F_o/\sigma(F_o)]_{min}$ excluded from refinement; N_{tot}, total number of reflections recorded; N_{indep}, number of independent reflections; N_{ref}, number of reflections included in refinement; N_{var}, number of refined variables; ρ_{res}, maximum residual electron density after refinement. The crystallographic calculations were performed with the program systems SDP (B. A. Frenz, Enraf-Nonius, Delft, Holland, 1978) and SHELX76 (G. M. Sheldrick, University of Cambridge, England, 1976).

This probably has to do with the fact that hydroquinone apparently has no possibility of establishing entirely satisfactory crystal packing as evidenced by its marked polymorphism (α, β, γ forms).[2] It is clear that the super-tetrahedral networks of Figs. 7(*a*), (*b*) created by the inter-(supra-) molecular combination of linear dialcohols and diamines should also be a favourable crystal-structural choice for linear amino alcohols H_2N–R^*_{di}–OH, such as *p*-aminophenol **5** and 4′-aminobiphenyl-4-ol **6**, which have their hydroxy and amino groups combined intramolecularly [Figs. 7(*c*), (*d*)]. X-Ray analyses of crystalline **5** and **6** have therefore also been undertaken; the resulting structures are described subsequently and their characteristics again turned out to be in line with our supramolecular design. It is noteworthy that a crude X-ray study of **5** was reported more than 40 years ago (photographic intensity estimates, incomplete refinements without consideration of H atoms, R = 0.19);[14] it is largely, yet not entirely, confirmed by our remeasurement as pointed out in the following section.

Experimental

Crystallizations

Commercial samples were used for the crystallizations, except 4′-aminobiphenyl-4-ol **6**, which was prepared from benzidine **4** by partial diazotization and subsequent hydrolysis. The 1:1 dialcohol–diamine molecular complexes **1·3**, **1·4**, **2·3** and **2·4** were grown from acetone at room temperature by dissolving equimolar amounts of the components and subsequent slow evaporation of the solvent. *p*-Aminophenol **5** was also crystallized from acetone at room temperature, **6** from ether. It is emphasized that the complex components and **5** were *dissolved* in acetone at room temperature, too, since heating easily leads to the formation of the Schiff bases between the amines and the solvent. This condensation reaction occurs to some extent even at room temperature and sometimes crystal mixtures were obtained. Obviously, the Schiff condensation is subject to acid catalysis, and the presence of the relatively acidic phenolic hydroxy groups may accelerate the reaction. It was found that addition of a small amount of triethylamine to the acetone solutions effectively quenches this acid catalysis leading to the desired crystals of the alcohol–amine molecular complexes and aminophenols, respectively, without complications. The double Schiff bases from the diamines and acetone are themselves capable of forming molecular complexes with hydroquinone **1** and 4,4′-dihydroxybiphenyl **2**. One example, *i.e.*, the 1:1 molecular complex (**1·7**) of hydroquinone **1** and the double Schiff base from *p*-phenylenediamine **3** and acetone, 1,4-bis-(isopropylideneamino)benzene **7**, was studied crystallographically in detail, and the results of the respective X-ray analysis are given in the Appendix. Samples of the complex crystals were redissolved and NMR spectra recorded in order to verify their composition and 1:1 stoichiometry.

X-Ray Analysis and Structure Refinement

The X-ray measurements were performed at room temperature on a four-circle diffractometer. Crystal data and details of the intensity measurements are collected in Table 1. All structures could be solved by conventional direct phasing methods without difficulties. The subsequent least-squares refinements likewise proceeded routinely and related data are included in Table 1. However, some comment is in order concerning one not entirely trivial point, that is the discrimination between oxygen and nitrogen atoms in the present crystal structures. This required some extra analytical efforts since the X-ray scattering power of oxygen and nitrogen is rather similar as the electron numbers of both atoms differ by one only, of course. The problem is thus in particular the distinction between hydroquinone **1** and *p*-phenylenediamine **3** in the crystals of their 1:1 complex **1·3**, and the identification of the analogous biphenyl systems **2** and **4** in **2·4**. Similarly, in the aminophenols **5** and **6**, the distinction between O and N establishes the orientation of the ON vector of these polar molecules in the crystal, *i.e.*, the direction of the molecular dipoles. Obviously, the problem of O,N distinction does not arise for the 'mixed' phenylene–biphenylene complexes **1·4** and **2·3**, for simple chemical reasons. Furthermore, it is clear that the assignment of O and N atoms is intrinsically related to the question of whether the crystal structures concerned are ordered or not. Now, in

Table 2 Comparison of some characteristic bond lengths, bond angles, torsion angles, hydrogen-bond lengths, and 'super-torsion angles' of the described super-tetrahedral molecular complexes and aminophenols[a]

Molecular system	**1·3**	**1·4**	**2·3**	**2·4**	**5**	**6**
d CO/Å	1.376	1.373	1.379	1.378	1.379	1.390
d CN/Å	1.431	1.422	1.433	1.432	1.440	1.432
∠CCO/°	122.9	122.9	122.3	122.4	122.4	121.9
	117.8	118.3	118.1	118.4	118.0	118.5
∠CCN/°	121.4	121.6	121.0	121.3	120.7	121.1
	120.0	120.9	120.2	120.3	120.0	120.2
∠HOCC/°	10	3	12	12	11	6
∠HNCC/°	−43	−48	−46	−46	−48	−51
	18	6	16	15	14	10
d ON(O–H···N)/Å	2.773	2.780	2.786	2.796	2.776	2.811
d ON(O···H–N)/Å	3.127	3.131	3.152	3.155	3.142	3.137
	3.254	3.225	3.282	3.220	3.259	3.314
∠O(H)N(H)O(H)N/°	62.2	63.7	63.5	64.2	62.5	63.5
	−58.6	−61.6	−62.8	−64.1	−64.2	−64.4
	56.5	56.2	54.8	54.9	55.4	55.3
	−64.0	−65.3	−64.8	−65.4	−62.8	−64.4
	57.7	60.7	61.9	63.1	62.5	63.3
	−47.0	−45.9	−45.6	−45.3	−47.5	−45.9

[a] The top CCO and CCN angles are defined within the more synplanar HOCC and HNCC torsion angles (Fig. 8). Of the latter, those with magnitudes > 90° are not given. The super-torsion angles are defined within the H-bonded super-cyclohexane rings and are given in cyclic order (see the text). Standard deviations are in the range of the last significant digits and may roughly be estimated with the help of Fig. 8.

short, all the six crystal structures discussed here turned out to be completely ordered within the experimental crystallographic data available, both as regards the N,O distribution and the location of the bridging H atoms in the hydrogen bonds. Given this, the discrimination between O and N in these X-ray analyses was based on the following five criteria. (1) Interchange of O and N leads to *R*-factor increases typically of about 0.03 in suitable test refinements. (2) The temperature motion of O and N is similar if correctly assigned; if not, the atom mistakenly chosen as O assumes an isotropic B_{iso} value typically 2 Å^2 larger than that of the atom wrongly assigned as N, with their sum amounting roughly to twice the correct value. (3) Difference Fourier electron density maxima around O and N corresponding to hydrogen atoms unambiguously support the assignment chosen, in line with the other criteria throughout. (4) The C–O bond length is consistently shorter than the C–N length, on average by 0.055 Å (Table 2, Fig. 8; average C–O and C–N lengths measured for the six crystal structures, 1.378 and 1.433 Å, respectively), in agreement with other structural evidence on phenols and aromatic amines. (5) The two phenolic CCO angles differ by 4–5°, the angle *syn* to the HOC angle being the larger one throughout, in accord with earlier observations;[15] on the other hand, the two amine CCN angles deviate by only 0.6–1.4° (Table 8, Fig. 8). Altogether, these criteria provide compelling evidence for the O,N assignments adopted in the present crystal structure analyses; a still more rigorous discrimination than is possible with X-ray methods would require neutron diffraction measurements. Based on these same criteria, no disorder was perceptible in the six crystal structures under discussion (see above), and this conclusion is further corroborated by a general crystal chemical, *i.e.*, supramolecular comparison of the two 'mixed' phenylene–biphenylene complexes **1·4** and **2·3** with the other structures (see below). Finally, it should be noted that the above N,O discrimination and disorder tests, when applied to *p*-aminophenol **5**, consistently indicated that the choice of oxygen and nitrogen in the old X-ray study of Brown[14] was the wrong one and is to be reversed.

Details of the present X-ray analyses and selected structural data are collected in Table 1 and Fig. 8; atomic coordinates and temperature factors have been deposited at the Cambridge Crystallographic Data Centre*. In Table 2, some characteristic geometrical data of the six crystal structures are grouped together for comparison. The atomic numbering, bond lengths, and bond angles, as well as certain temperature motion properties may be found in Fig. 8. Figs. 9 and 10 present packing diagrams and characteristic supramolecular architectures of the individual structures.

Results and Discussion

Space Group and Molecular Symmetries

The four diphenol–diamine complexes **1·3**, **1·4**, **2·3** and **2·4** all crystallize in the centrosymmetric space group $P2_1/c$ with two formula units of complex in the unit cell (Table 1). Therefore, the molecular components of these complexes are all centrosymmetric in the crystal. This might have been expected for hydroquinone **1** and *p*-phenylenediamine **3**, since molecules centrosymmetric in the gas phase have a general propensity to retain this symmetry in the crystal.[16] The (average) crystallographic centrosymmetry of the biphenyl systems **2** and **4** is less trivial and implies effective planarity of these molecules, whereas, in the gas phase, non-centrosymmetric, non-planar structures twisted around the central C–C bond have to be reckoned with (see the section on Molecular Structure).

The two non-centrosymmetric, polar aminophenols **5** and **6** both crystallize in the likewise non-centrosymmetric, polar space group $Pna2_1$, with four molecules in the unit cell. Therefore, **5** and **6** have no crystallographic molecular symmetry, and no further structural conclusions may be drawn. Nonetheless, from the X-ray analysis the biphenyl compound **6** also turned out to have an essentially planar structure in the crystal. It is briefly anticipated at this point that a comparison of the cell constants of the six crystal structures under discussion (Table 1) would reveal striking similarities and regularities among the shapes of their unit cells. Clearly, this reflects close structural relationships between the six crystal architectures, and we shall come back to this more relevant point of our comparative supramolecular analysis in the section on Supramolecular Structure.

* For details of the CCDC deposition scheme, see 'Instructions for Authors (1994),' *J. Chem. Soc., Perkin Trans. 2*, 1994, issue 1.

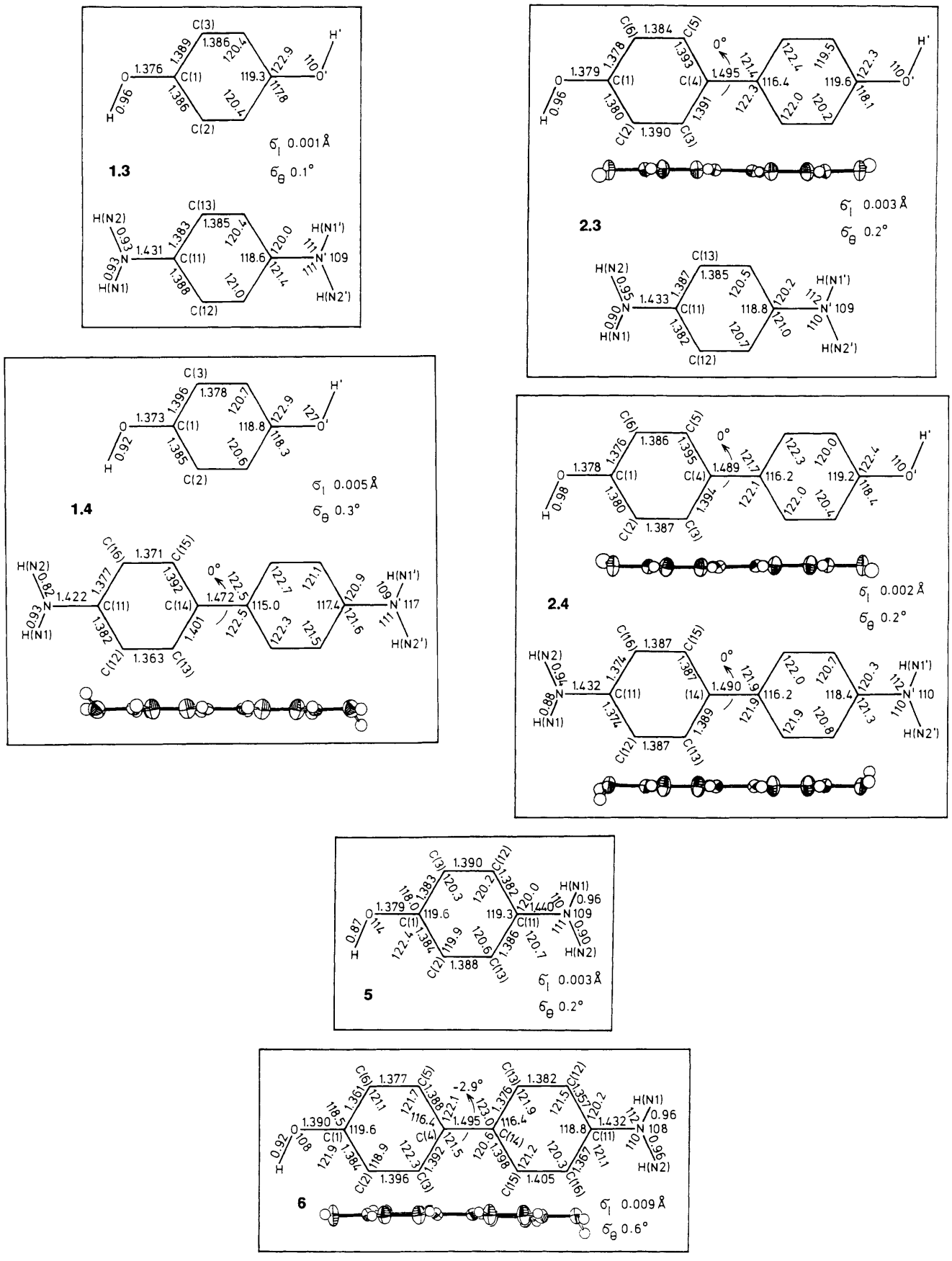

Fig. 8 Molecular structural data and atomic numbering of the diphenol–diamine complexes **1·3**, **1·4**, **2·3** and **2·4**, and the aminophenols **5** and **6**: bond lengths (Å), bond angles (deg), twist angle around central C–C bond of biphenyl systems; average estimated standard deviations of heavy-atom bond lengths (σ_1) and angles (σ_θ). For the biphenyl systems **2**, **4** and **6**, side views with heavy-atom anisotropic vibrational ellipsoids of 50% probability are shown (isotropic temperature factors of H-atoms divided by 3).

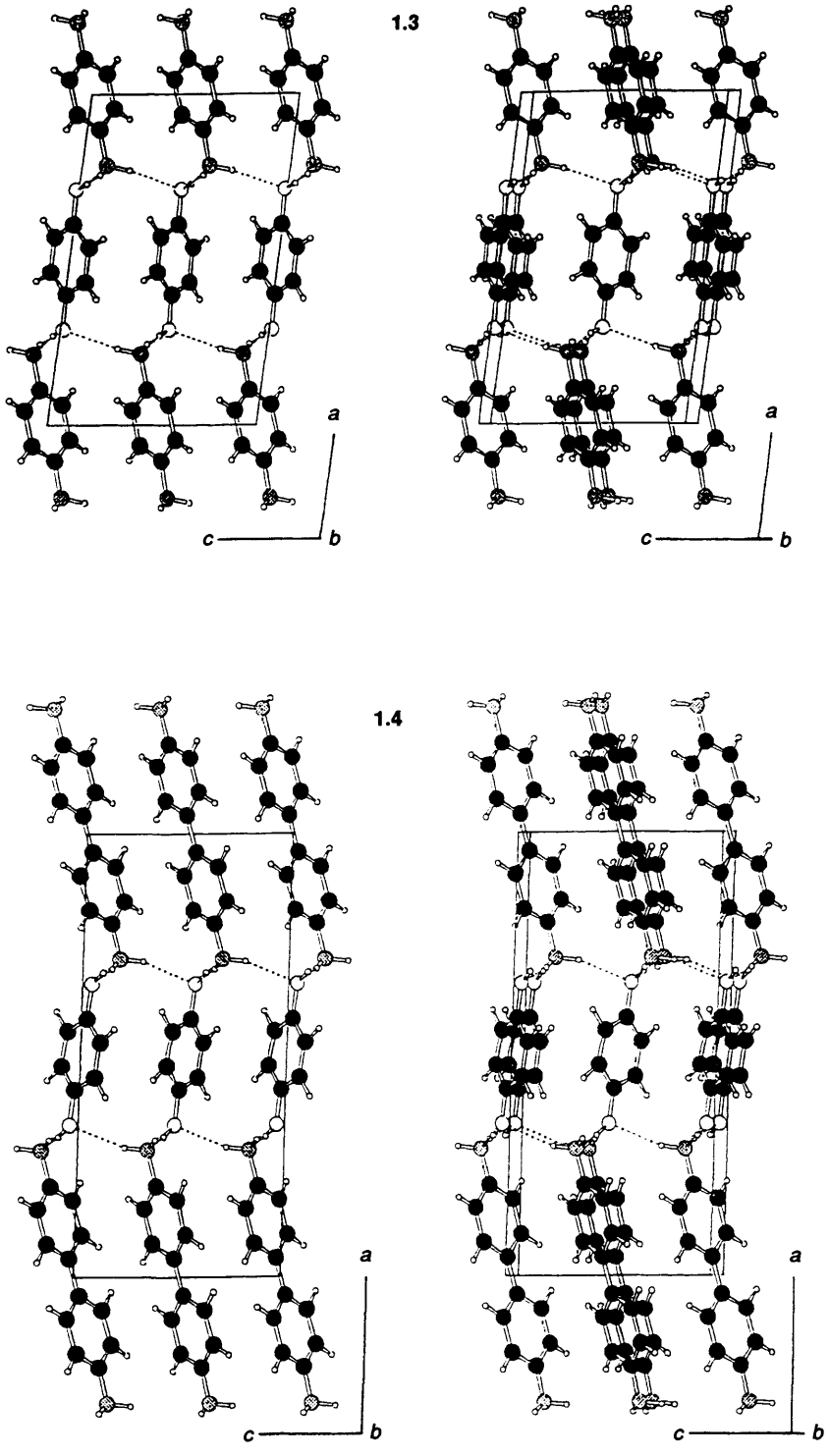

Fig. 9 (*contd.*)

Molecular Structure

The intramolecular geometries of the molecules **1**–**6** making up the six crystal structures compared in this work are rather unexceptional and only a few points merit explicit comment. Numerical data substantiating the following discussion may be found in Table 2 and Fig. 8. Since both the intra- and intermolecular geometrical details of the various structures are strikingly similar, it is not necessary to analyse them individually but rather in summary.

The C–O bond lengths in the six crystal structures are normal (average 1.378 Å) and compare well with those of hydroquinone[2,15] and phenol (gas-phase value 1.374 Å[17]). However, the C–N bonds in the present structures (average length 1.433 Å) are somewhat longer than in crystalline and gaseous *p*-phenylenediamine (averages 1.409,[18a] 1.416,[18b] and 1.424 Å,[18b] respectively), or in gaseous aniline (1.402 Å[19]). Hydrogen bonding may be influential inasmuch as in the present structures the nitrogen lone pairs are involved in a relatively short O–H • • • N bond (average ON distance 2.787 Å) and are thus not fully available for π overlap with the aromatic ring. In crystalline *p*-phenylenediamine the weaker N(H)N bonds are all longer than 3.2 Å.[18] Furthermore, for the same reason the bonding geometry at the nitrogen atoms is more pyramidal in the present cases than in *p*-phenylenediamine and aniline. The crystal structural study of a complex, say, between hydroquinone and aniline (1 : 2) would be helpful to check this reasoning. The central C–C bond linking the two benzene rings of the present biphenyl systems is about 0.02 Å longer (average

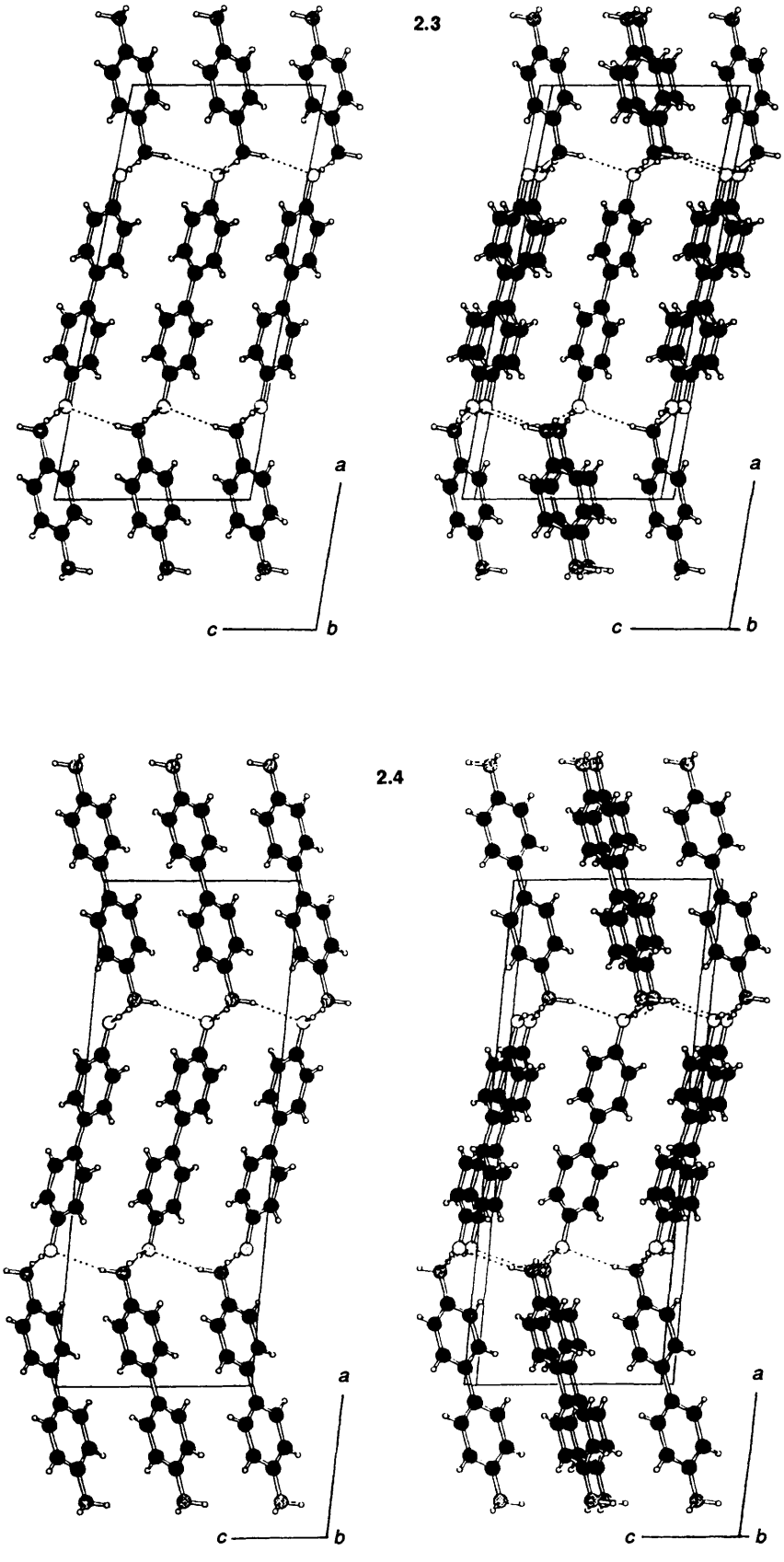

Fig. 9 (*contd.*)

1.488 Å) than a normal $C(sp^2)$–$C(sp^2)$ single bond owing to the inner non-bonded H • • • H repulsions (see below).

The CCO and CCN bond angles in the present structures merit a short comment. Their differences were used as a criterion to discriminate between O and N in the structure refinements as detailed in the Experimental section. The CCO angles a in *syn* disposition with respect to the COH angles are, on average, 4.4° larger than their *anti* partners. The effect has been noted earlier;[15] in the planar gaseous phenol molecule this angular difference amounts to 5.1°.[17] For obvious symmetry reasons, the corresponding CCN angular difference is much smaller (average 0.9°) but consistently the CCN angle involved

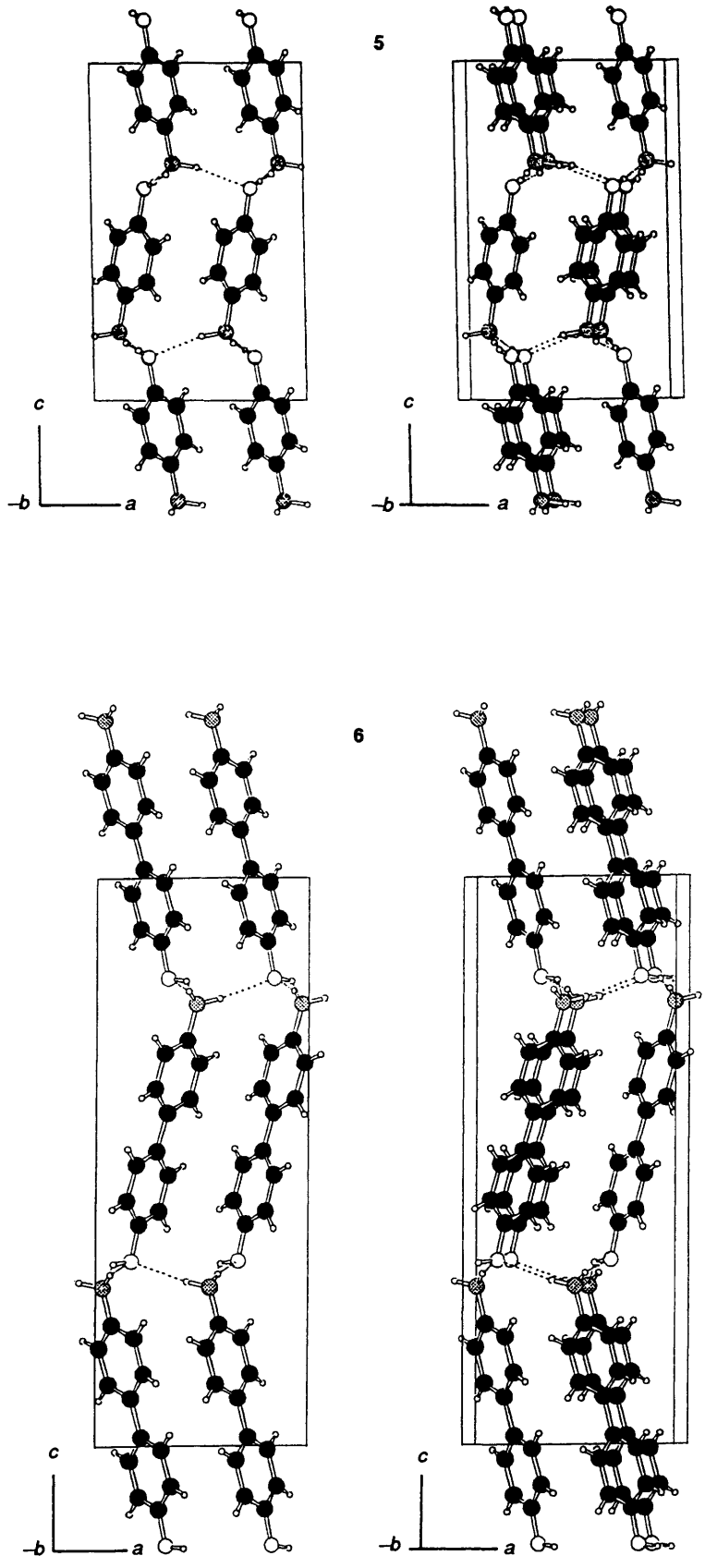

Fig. 9 Stereo packing diagrams of diphenol–diamine complexes and aminophenols with cell edges outlined: O, white; N, grey; C, black; H-bonds dotted. For all left-handed members of the stereo pairs, the view is along the short cell edge *b* (*ca.* 5.3 Å) defined by a 1,3 distance of the puckered H-bonded super-arsenic sheets.

in the smaller (roughly synplanar) CCCN torsion angle is again the larger one.

As regards the torsional structure of the present phenols and amines, two topics are highlighted, that is the planarity of the biphenyl systems and the conformations of the hydroxy and amino groups. The torsional structure of biphenyl has been the

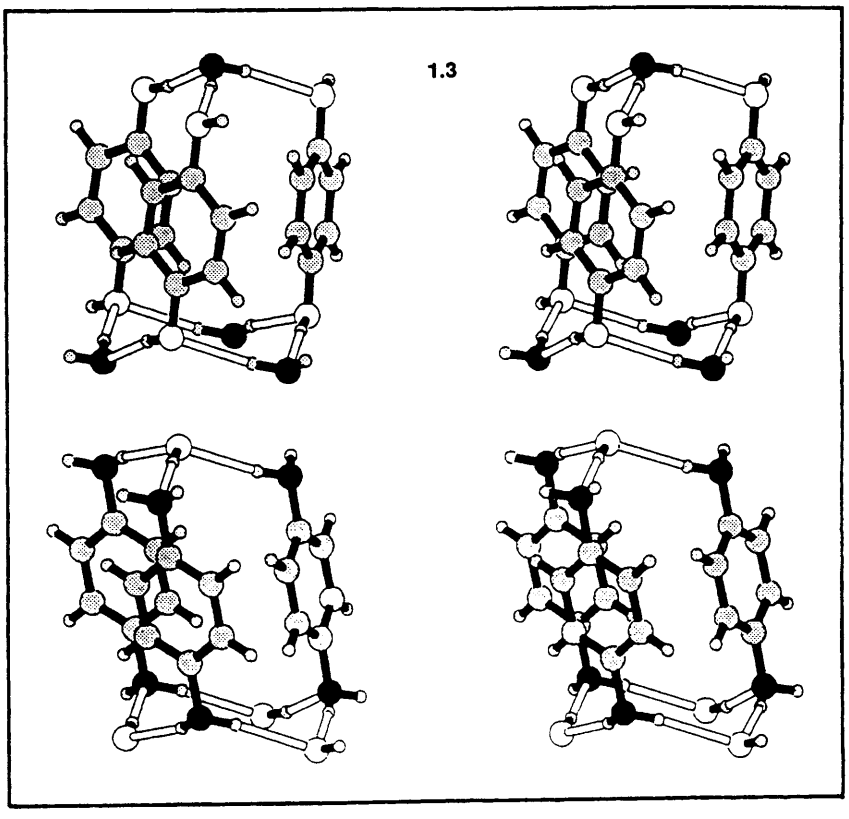

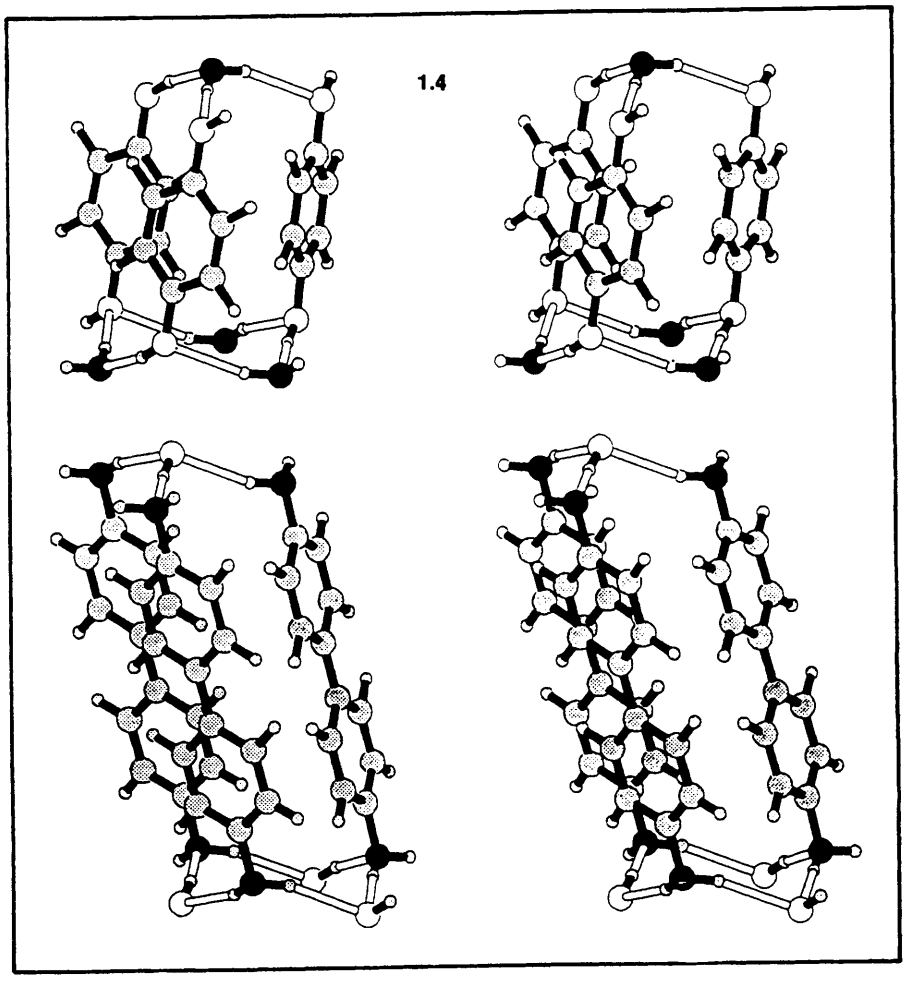

Fig. 10 (*contd.*)

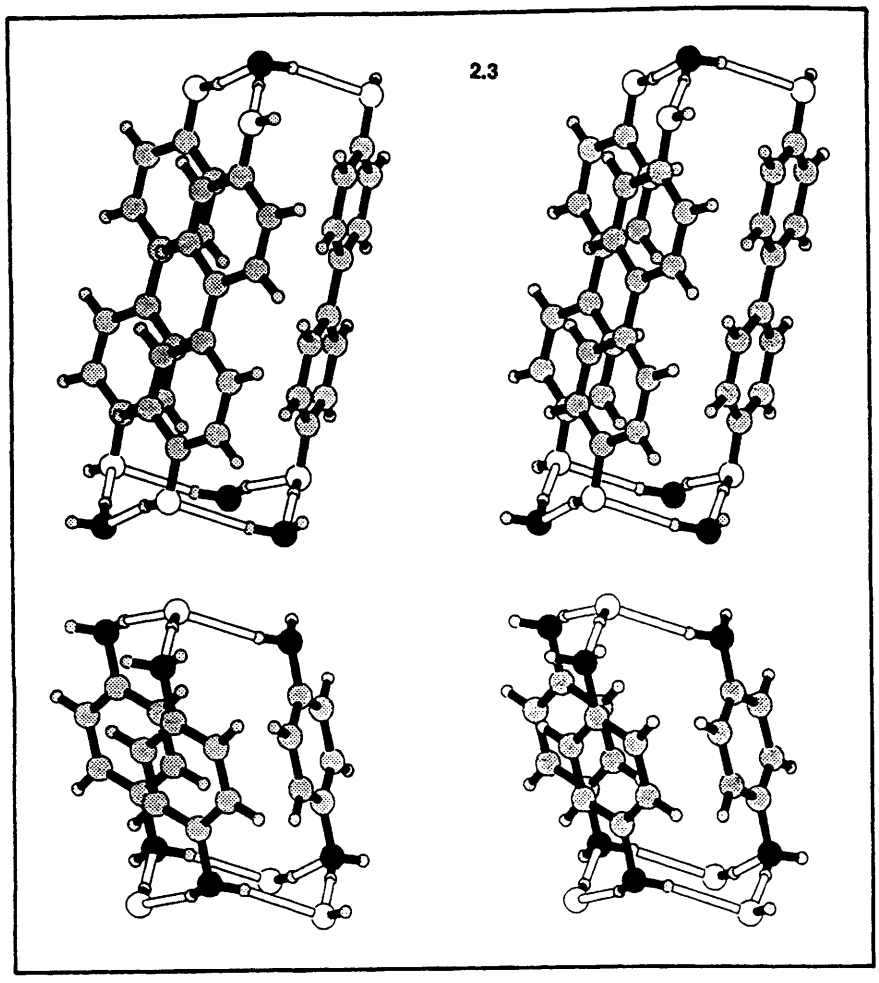

Fig. 10 (*contd.*)

subject of numerous experimental and theoretical studies[20a] since it depends on a subtle balance between π overlap of the benzene rings (favouring planarity) and the inner non-bonded H···H repulsions (favouring a non-planar structure twisted about the central C–C bond). The two opposing effects almost cancel each other. In the gas phase, biphenyl has a non-planar structure of D_2 symmetry with the two benzene rings twisted about the central C–C bond by *ca.* 45°[20a] whereas in the crystal at room temperature the molecule is (on average) centrosymmetric (space group $P2_1/c$ with two molecules in the unit cell) indicating effective planarity. Temperature motion analysis yields relatively large librational motion about the central C–C bond, however, which may, in fact, correspond to a double-minimum twisting potential such that the crystal structure would be disordered and consist of a statistical mixture of twisted molecules executing low-energy high-amplitude twisting vibrations across a shallow barrier, *i.e.*, a planar transition state.[21] At 40 K, biphenyl undergoes a phase transition leading to a non-centrosymmetric crystal structure, and at 22 K a twist angle of about 10° was measured by neutron diffraction.[20b] A number of substituted biphenyls (excluding *ortho* substitution) were found to behave largely alike.[20c]

In the four present crystal structures involving biphenyl systems, *i.e.*, **1**·**4**, **2**·**3**, **2**·**4** and **6**, the heavy-atom skeletons of these molecules are effectively planar. In the three molecular complexes, crystallographic centrosymmetry is imposed (see the above section on Space Group and Molecular Symmetries), which implies untwisted structures and, together with the observed trigonal planar bonding at the sp^2 carbon atoms, planarity. Inspection of the anisotropic temperature motion, *i.e.*, the atomic vibrational ellipsoids shown in Fig. 8, suggests some enhanced, but not excessive, torsional motion around the central C–C bonds of **2** and **4**, such that, all in all, it appears appropriate to refer to them as virtually planar. Clearly, this reasoning strictly applies only to *average* structures and symmetries, and subtle disorder effects in terms of torsionally interconverting, slightly twisted structures cannot be rigorously ruled out. No crystallographic symmetry is imposed on 4′-aminobiphenyl-4-ol **6**, which is nevertheless also observed to be essentially planar in the crystal (twist angle around the central C–C bond 2.9°). There is room for the belief that biphenyl planarity is stabilized in the present cases by crystal packing forces, *i.e.*, by the stacking of the aromatic rings and hydrogen bonding constraints, but quantitative evidence supporting this assumption is hard to produce from our data. As noted above, planarity of crystalline biphenylene itself is also supported by packing forces, and the stacking of the molecules is similar to that of the biphenylylene units in our present cases (see below). Finally, the direct intramolecular influence of the substituents in our biphenyl derivatives is difficult to assess without quantitative calculations.

The phenolic OH groups in the present crystal structures lie approximately in the plane of the benzene rings and the maximum deviations of the HOCC torsion angles from planarity amount to 12° (average 9°, Table 8). This may be compared with the phenol molecule, which, in the gas phase, is completely planar.[17] Likewise, the conformation of the amino groups in the present structures is roughly similar to that in aniline, which in the gas phase involves a mirror plane running perpendicular to the benzene ring and bisecting the NH_2 group.[19] On average, the amino groups of the present molecules are rotated out of this symmetric arrangement by a maximum

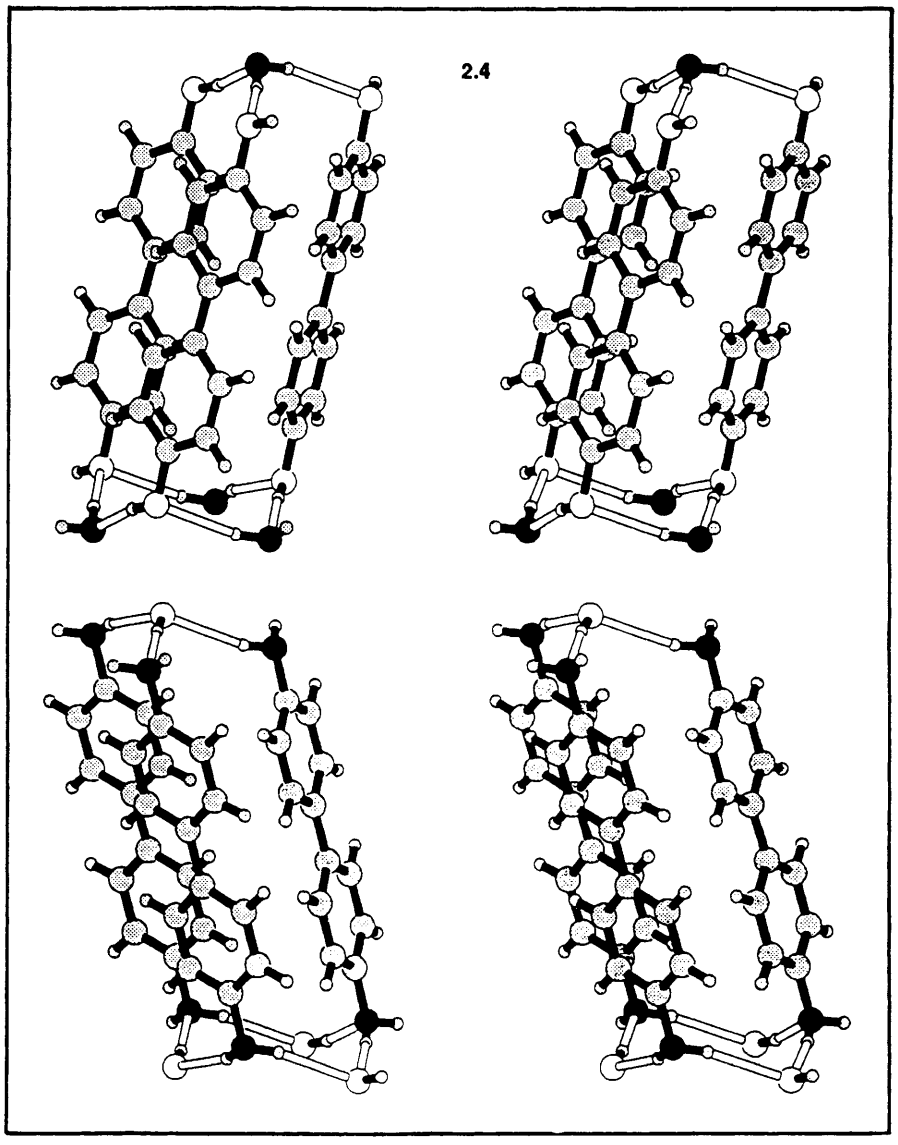

Fig. 10 (*contd.*)

of 21° (averaged 17°, Table 8). Obviously, these conformational deviations from ideal mirror symmetries are dictated by packing requirements such as favourable hydrogen bonding and efficient stacking of the aromatic residues.

Supramolecular Structure

The four linear dialcohol–diamine molecular complexes **1**·**3**, **1**·**4**, **2**·**3**, **2**·**4**, and the two linear aminophenols **5** and **6** build up the expected (see the Introduction) super-tetrahedral H-bonded architectures in the crystal. In the perfectly ordered crystal structures, every O and N atom is engaged in 3 H bonds with approximately tetrahedral coordination. In all six cases, exclusively O(H)N bonds are observed. *i.e.*, each oxygen atom is H-bonded to three nitrogen atoms, and each nitrogen atom to three oxygen atoms. The hydrogen bonds are arranged in all-*trans* fused 'super-cyclohexane' chairs, which form infinite H-bonded 'super-arsenic' sheets [Fig. 5(*b*)] held together by the covalent *p*-phenylene and *p*,*p*′-biphenylylene bridges (spacers). The puckered H-bonded sheets are, in all respects, very similar structurally (Table 2, Figs. 9–11). In all cases, we have three crystallographically independent O(H)N bonds, one O–H···N and two O···H–N bonds, as stoichiometrically required. The H-bonds of the former type are relatively short (average ON distance 2.787 Å), those of the latter type rather long (average ON distances 3.141 and 3.292 Å; Table 2). The degree of puckering of the H-bonded super-arsenic sheets may be quantified by the O(H)N(H)O(H)N 'super-torsion angles' of the super-cyclohexane chairs, whose values averaged over the six crystal structures are in cyclic order 63.3, −62.6, 55.5, −64.5, 61.5, −46.2° (Table 2; note the strikingly close similarity of the individual values). It is readily seen that these super-torsion angles satisfy fairly well D_{3d} and closely C_2 chair ring symmetry. Furthermore, their roughly synclinal magnitudes imply approximately tetrahedral N(H)O(H)N and O(H)N(H)O angles on average, and thus the super-cyclohexane chair ring pucker of the H-bonded super-arsenic sheets happens to be similar to that of cyclohexane itself.

The extensive supramolecular similarities and regularities among the present six super-tetrahedral crystal architectures are already expressed rather conspicuously through the dimensions of their crystallographic unit cells (Table 1). It may be seen that all these cells have a similar small edge of about 5.3 Å length and a similar medium edge about 8.1 Å long. These lengths are determined by the dimensions of the H-bonded super-arsenic sheets, and correspond to 1,3 and 1,5 distances within the fused super-cyclohexane architectures as illustrated in Fig. 11. The large cell edges may be grouped into three pairs of about 13.0, 17.2 and 21.3 Å length. They are essentially brought about by the width of the H-bonded super-arsenic

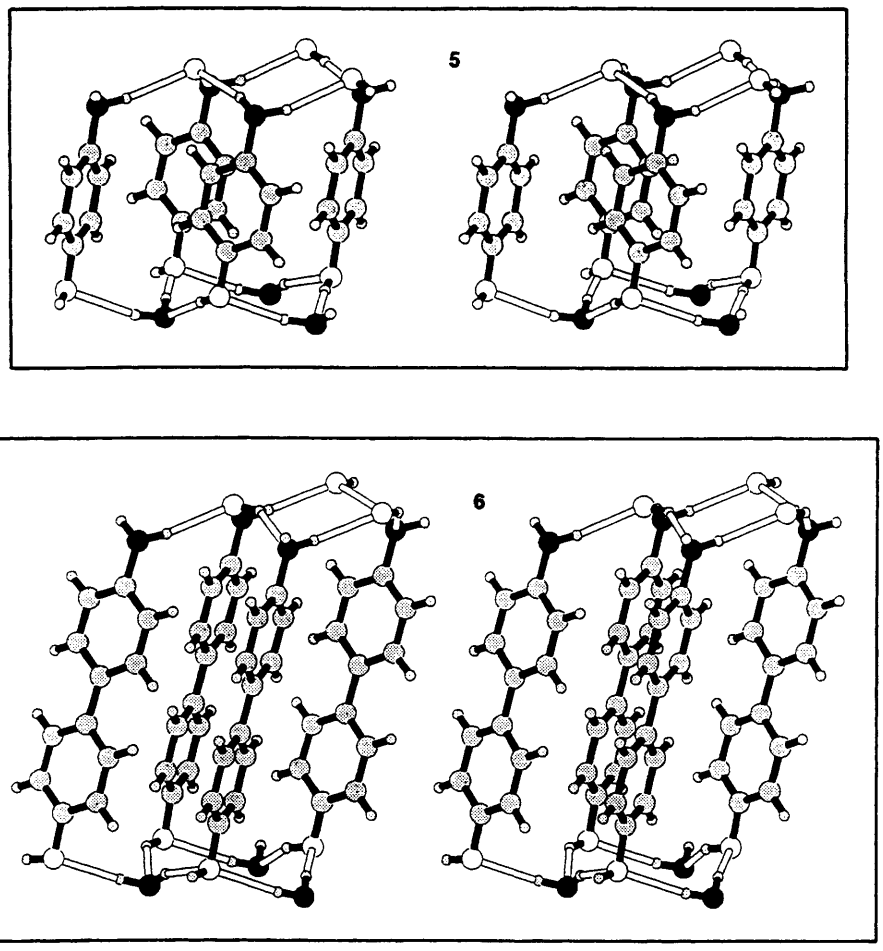

Fig. 10 Stereo views of the super-adamantane building blocks of the complexes **1·3**, **1·4**, **2·3** and **2·4**, and the fused super iceane/super-bicyclo-[2.2.2]octane units of **5** and **6** as cut out of the H-bonded super-diamond and super-wurtzite networks, respectively: O, white, N, black, C, grey; H-bonds represented as open rods. In the complexes, two different super-adamantane units occur, depending on whether the *p*-phenylene and *p*,*p*′-biphenylylene spacers involved belong to the diphenol (top) or the diamine partner. Note that the long axes of the aromatic spacers do not run exactly orthogonal to the mean planes of the H-bonded sheets, but are tilted away from orthogonality at the O and N atoms in opposite directions (see the text for details concerning these distortions).

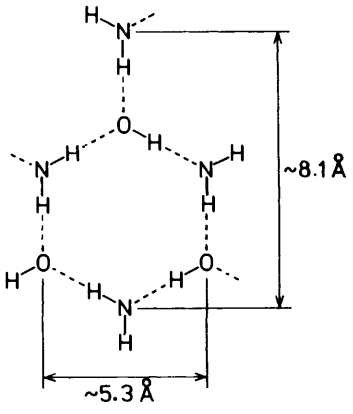

Fig. 11 Interpretation of the small and medium unit cell edges of the complexes **1·3**, **1·4**, **2·3** and **2·4**, as well as **5** and **6**, in terms of the dimensions of the puckered H-bonded sheets. The larger cell edges are determined by the length of the aromatic spacer bridges protruding roughly (but not exactly) at right angles from the H-bonded sheets, and by the latter's thickness.

sheets (*ca.* 1.00 Å) and the length of the *p*-phenylene and *p*,*p*′-biphenylylene spacers linking them. These spacer lengths may be approximated as multiples of an average bond length of *ca.* 1.38 Å, and, with the help of Fig. 9, it may be seen that the lengths (in Å) of the large cell edges are reproduced rather well by the expression $2 \times 1.00 + 8 \times 1.38 + 3n \times 1.38 = 2.00 + (8 + 3n) \times 1.38$, where n equals 0,1,2 depending on whether the spacers are exclusively *p*-phenylene as in **1·3** and **5**, alternately *p*-phenylene and *p*,*p*′-biphenylylene as in **1·4** and **2·3**, or exclusively *p*,*p*′-biphenylylene as in **2·4** and **6**. Note that this geometric analysis does not account for the fact that the long axes of the spacers are not exactly orthogonal to the mean plane of the H-bonded super-arsenic sheets (see below) and that the cell edges of the monoclinic complexes are of course not all exactly orthogonal; ensuing corrections are small, however. As detailed further below, it so happens that the steric requirements for satisfactory hydrogen bonding in the puckered super-arsenic sheets and favourable lateral stacking of the aromatic spacers comply well with each other, as is required, of course, for an energetically favourable overall crystal packing.

The very similar super-tetrahedral H-bonded crystal architectures of the four linear diphenol–diamine complexes **1·3**, **1·4**, **2·3** and **2·4** are distorted cubic-diamond-like or zinc-blende-like, those of the linear aminophenols **5** and **6** distorted hexagonal-diamond-like or wurtzite-like (Figs. 7, 9, 10). The wurtzite analogy of the latter is closer than the zincblende relationship of the former, since, in the crystals of **5** and **6**, every oxygen atom is indeed tetrahedrally coordinated to four nitrogen atoms and every nitrogen atom to four oxygen atoms [three times *via* O(H)N hydrogen bonds, once *via* the covalent aromatic bridge]; in the diamondoid complexes every oxygen atom is coordinated to three nitrogen atoms and one oxygen atom, and every nitrogen atom to three oxygen atoms and one

nitrogen atom. Fig. 10 provides views of characteristic building blocks cut out of the super-tetrahedral networks, *i.e.*, super-adamantane units to represent the super-diamond architectures, and fused super-iceane/super-bicyclo [2.2.2]octane units to represent the super-wurtzite networks. (As regards the trivial name 'iceane' attached to tetracyclo[5.3.1.$1^{2,6}$.$0^{4,9}$]dodecane, note that normal hexagonal ice builds up a super-wurtzite network; *cf.* the Introduction.)

The diamondoid nature of the crystal architectures of the diphenol–diamine complexes and, in particular, the wurtzite-like crystal structures of the aminophenols are also expressed by comparing the associated space-group symmetries. The space group of the former, $P2_1/c$, is a (remote) subgroup of that of cubic diamond, $Fd\bar{3}m$, while the space group of the latter, $Pna2_1$, is a maximal non-isomorphous subgroup of that of wurtzite, $P6_3mc$.[22] (Note that the wurtzite space group is in turn a subgroup of $P6_3/mmc$ applying to hexagonal diamond.) On the other hand, $P2_1/c$ is not a subgroup of the non-centrosymmetric zincblende space group $F\bar{4}3m$. ($F\bar{4}3m$ is of course a subgroup of the diamond space group $Fd\bar{3}m$.) Thus the crystallographic molecular centres of symmetry of the diphenol–diamine complexes are the only remaining point-group symmetries of the diamond lattice, *i.e.*, a quarter of diamond's symmetry centres located on the midpoints of the C–C bonds. On reducing the crystal symmetry of wurtzite to that of the aminophenols no point group symmetry is conserved.

It is of some interest to reflect briefly on the abovementioned distortions of the H-bonded super-diamond and super-wurtzite networks in the diphenol–diamine complexes and aminophenols, respectively, relative to the ideal geometries of diamond and wurtzite themselves. Clearly, the present supramolecular lattices are elongated along former threefold axes of diamond and wurtzite since the covalent aromatic spacer bridges are longer than the O(H)N distances of the hydrogen bonds. A second, more interesting mode of distortion refers to the fact that the long axes of the aromatic spacers, *i.e.*, the vectors interconnecting the two hetero atoms, do not run exactly orthogonal to the mean planes of the puckered H-bonded super-arsenic sheets, but in all cases are tilted away from orthogonality by typically 10–15° (Figs. 9, 10). The tilt essentially corresponds to a rotation about the short crystallographic *b* axis by this amount. Inspection of the Figures reveals that the tilts at oxygen and nitrogen are always opposite in the sense that in all cases at the oxygen atoms the aromatic bridges are tilted outward away from the interior of an H-bonded super-cyclohexane ring, while at the nitrogen atoms, a corresponding inward tilt toward an $(OHNH)_3$ ring interior is always observed. Probably, the tilt phenomenon has to do with how the aromatic spacers pack together in their layers between the H-bonded super-arsenic sheets. This aromatic stacking follows a herring-bone pattern with edge-to-face (ETF) contacts among neighbouring aromatic systems. The observed tilting distortion ensures that aromatic H-atoms roughly assume a (favourable) position above the interior of a benzene ring of an ETF disposed neighbouring molecule (Figs. 9, 10). It is interesting to note that the corresponding packing characteristics of the parent hydrocarbons benzene[23] and biphenyl[24] are exactly alike.[25] However, we have no convincing explanation to offer as regards the *opposite* direction of tilting at the oxygen and nitrogen atoms, respectively.

The question arises as to why the four diphenol–diamine complexes **1·3**, **1·4**, **2·3** and **2·4** choose to build up super-diamond architectures in the crystal, whereas the two aminophenols **5** and **6** prefer the super-wurtzite alternative. An explanation of this different supramolecular behaviour is not obvious, since both packing modes are expected to be energetically very similar. (Note that hexagonal diamond is only about 1.5 kcal mol^{-1} less stable than cubic diamond.) That the four molecular complexes aggregate in diamondoid fashion appears empirically plausible since they are made up of centrosymmetric molecules, which generally tend to preserve this symmetry in the crystal (see the section on Space Group and Molecular Symmetries). Obviously, centrosymmetry may only be kept in a diamondoid network, not in a polar wurtzite-like architecture. But why are the H-bonded super-arsenic sheets in the two aminophenol crystals connected wurtzite-like and not zincblende (diamond)-like by the aromatic spacer bridges? A partial answer may possibly be provided by the following line of arguments. It was noted above that the aromatic spacer bridges experience a tilt with respect to the normal of the planes of the H-bonded sheets in order to improve the edge-to-face stacking within the aromatic layers, and that this tilt is always opposite at oxygen and nitrogen. Whatever the deeper reasons for these opposing orientational preferences at oxygen and nitrogen may be, it is immediately clear that in case of the aminophenols they may only be satisfied within a wurtzite-type lattice, since here the tilting distortion is anti-symmetric with respect to the mean plane through the aromatic layers. In the diphenol–diamine complexes, on the other hand, the tilting direction at both ends of the spacer bridges is the same, which is only ensured in a diamond-type lattice, since here the tilting distortion is symmetric with respect to the aromatic symmetry centres. Thus it appears possible that the opposite tilting preferences at oxygen and nitrogen determine whether a super-zincblende or a super-wurtzite network is built up. Another possibility could be that the super-wurtzite and super-zincblende supramolecular alternatives, respectively, of our systems exist as energetically similar polymorphs; variable temperature studies would be required to settle this question.

The supramolecular H-bonded crystal architectures of the aminophenols **5** and **6** are the first organic examples of super-wurtzite structures, counting, for example, the stable form (I_h) of ice or the SiO_2 polymorph tridymite as inorganic representatives. A partly organic case of a large H-bonded super-wurtzite network is discussed in the following section on Related Structures. It may generally be stated that large super-wurtzite architectures are rare, whereas many examples of the super-diamond alternative are, by now, known. This holds in particular for multiple, interpenetrating super-tetrahedral networks,[11] which are diamondoid in all cases studied so far. Why is this so? In the case of single networks there is little to argue in favour of either one of the two alternatives, which should occur with about equal abundance. The small energetic differences between the diamondoid and wurtzite-like structures of ice (ice-I_c, ice-I_h), SiO_2 (crystobalite, tridymite), and also of carbon (cubic diamond, hexagonal diamond; see above) and ZnS (zincblende, wurtzite) themselves may serve to support this expectation. Solid-state inclusion compounds with single super-tetrahedral host lattices based on $Cd(CN)_2$,[26,27] metal complexes of tetrahedral tetranitriles,[27] and tetrahedral tetralactams[28] have recently been described, which are all diamondoid. This might also be due to the guest species inasmuch as it seems conceivable that a super-wurtzite framework is more shape-demanding towards molecular guests since it involves two types of cage (50% larger super-iceane, 50% smaller super-bicyclo[2.2.2]octane cavities), whereas a super-diamond host has exclusively (medium-sized) super-adamantane cages. (But note, however, that a super-zincblende network with two different types of tetrahedral centre has, likewise, two different kinds of super-adamantane cage!) On the other hand, the fact that multiple, (self-) interpenetrating super-wurtzite networks have never been observed, may readily be rationalized in terms of simple but stringent symmetry requirements: the iceane and bicyclo[2.2.2]octane cages of the wurtzite lattice have only trigonal symmetry (ideally D_{3h}), whereas the local symmetry of the tetravalent lattice points is

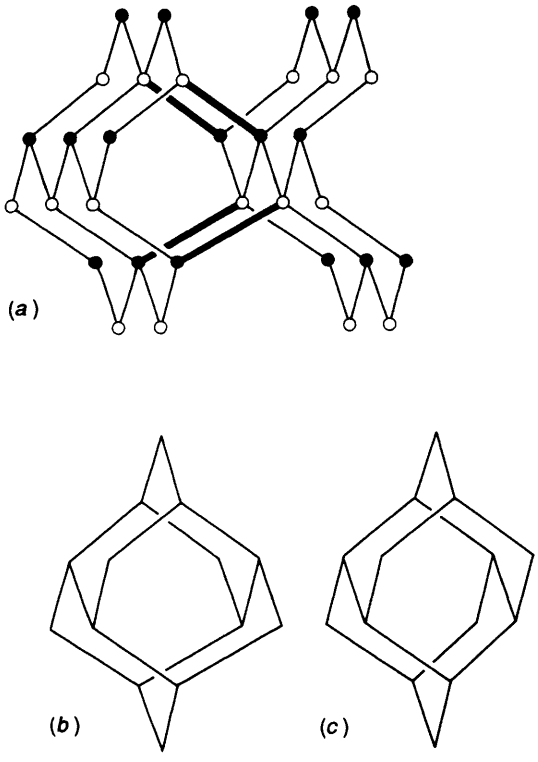

Fig. 12 (*a*) Super-tetrahedral H-bonded 3D network of crystalline ethanolamine, $HOCH_2CH_2NH_2$ (diagrammatic, based on X-ray data of ref. 31). O, white, N, black spheres; O(H)N hydrogen bonds drawn as thin lines, covalent ethylene linkers, $-CH_2CH_2-$, as thick black rods. The H bonds span 'super-black phosphorus' sheets with *cis*-decalin-like structural elements, which are covalently bridged by the ethylene linkers in non-diamondoid fashion (non-equivalent ON distances of the H-bonds, 2.785, 3.138, 3.282 Å[31]). (*b*) Skeleton of hypothetical D_2 symmetric 'isodiamantane' (pentacyclo-[8.4.0.0^{3,8}.0^{5,14}.0^{7,12}]tetradecane), which may be cut out of the H-bonded ethanolamine network and represents its characteristic building block. (*c*) Skeleton of D_{3d} symmetric diamantane (pentacyclo-[7.3.1.1^{4,12}.0^{2,7}.0^{6,11}]tetradecane).

tetrahedral (ideally T_d), such that self-interpenetration is hardly possible; for extremely large networks this might perhaps not hold, but even then the degree of interpenetration should be limited. In contrast, the lattice points and adamantane cages of the diamond lattice have the same symmetry (T_d) and self-interpenetration of super-diamond networks is readily possible. A similar case in point is the octahedral cubic primitive polonium (or ReO_3) lattice whose hexavalent lattice points and cube-shaped cages have the same symmetry (O_h) thus permitting supramolecular self-interpenetration. Multiple, interpenetrating super-octahedral networks are present in β-hydroquinone and related inclusion compounds,[2] Nb_6F_{15},[29] and $Ag_3Co(CN)_6$[30] with double, double and triple (distorted) super-polonium networks, respectively.

Related Structures

The crystal structure of ethanolamine, $HOCH_2CH_2NH_2$, has recently been reported[31] but no description of the type of hydrogen-bonded network adopted in the crystal was given. Not unexpectedly, a closer look at this architecture reveals it to be (distorted) super-tetrahedral, but in a novel fashion. As in our present cases, exclusively O(H)N hydrogen bonds are formed, 1.5 each per oxygen and nitrogen atom, which, however, do not span super-arsenic but super-black phosphorus sheets [Fig. 5(*c*)]. These sheets with partially *cis*-fused super-cyclohexane chairs are bridged covalently by the ethylene units, $-CH_2CH_2-$, to form a single three-dimensional super-tetrahedral network, yet not in diamondoid fashion. The characteristic building block of this network corresponds to the twisted carbon skeleton of hypothetical pentacyclo-[8.4.0.0^{3,8}.0^{5,14}.0^{7,12}]tetradecane ('isodiamantane', symmetry D_2), which might be related to that of diamantane (D_{3d}) as shown in Fig. 12. As in the aminophenols **5** and **6** with wurtzite-like H-bonded networks, every oxygen atom of ethanolamine is coordinated to four nitrogen atoms and *vice versa*, such that we might refer to the H-bonding pattern of $HOCH_2CH_2NH_2$ as 'isozincblende'-like. We are not aware of another example of this new variant of a 3D 4-connected network.

Given the super-tetrahedral 3D network of ethanolamine brought about by forming the maximum possible number of hydrogen bonds, 1:1 complex formation between ethyleneglycol, $HOCH_2CH_2OH$, and ethylenediamine, H_2NCH_2-CH_2NH_2, may be expected and again a supertetrahedral, probably also 3D 4-connected network foreseen in the crystal. We have not studied this system as yet, which would require low-temperature crystallizations and X-ray intensity measurements. Support in favour of complex formation between ethyleneglycol and ethylenediamine may be derived from the simple observation that mixing of the two liquids is accompanied by very substantial heat evolution.

As a lower homologue of ethanolamine, hydroxylamine, $HONH_2$, the simplest possible amino alcohol, is, of course, also a potential candidate as regards the creation of a H-bonded super-tetrahedral network. X-Ray crystallographic evidence on hydroxylamine[32] indeed bears out this conjecture. Hydroxylamine forms a single 3D 4-connected network in the crystal consisting of undulating H-bonded sheets linked by covalent O–N bonds (Fig. 13). Every oxygen atom is H-bonded to three nitrogen atoms and *vice versa*, in a rather distorted tetrahedral fashion. Thus again exclusively O(H)N hydrogen bonds occur. The H-bonded sheets consist of fused distorted super-cyclohexane boats, and are connected by the covalent O–N bonds, in a mode which is neither diamond- nor wurtzite-like. Again we are not aware of any other example with this type of network.

We conclude this section with a brief discussion of the only other chiefly organic super-wurtzite architecture known (to us). It occurs in a formal 1:1 complex between ammonium tetrafluoroborate and urotropin, $NH_4BF_4 \cdot (CH_2)_6N_4$, the crystal structure of which was determined some time ago[33] yet not analysed as regards packing and supramolecular structure. The super-wurtzite network is undistorted in this case and brought about by super-tetrahedral N(H)N hydrogen bonding between the tetrahedral ammonium cations and the tetrahedral urotropin molecules, which are readily seen to enjoy a relationship of perfect H-bond donor–acceptor complementarity. The symmetry characteristics of this super-wurtzite network are exactly the same as those of wurtzite itself, *i.e.*, the crystallographic space group is, in both cases, $P6_3mc$ with two formula units in the unit cells. Transforming both crystal architectures into one another simply requires replacement of Zn^{2+} by NH_4^+ and of S^{2-} by $(CH_2)_6N_4$, or *vice versa*. Each super-iceane cage of the cationic H-bonded $NH_4^+ \cdot (CH_2)_6N_4$ super-wurtzite network houses a BF_4^- anion, while the super-bicyclo[2.2.2]octane cages are essentially filled up by their own constituents without leaving empty spaces (Fig. 14). $NH_4BF_4 \cdot (CH_2)_6N_4$ therefore has the characteristics of a solid-state host–guest inclusion compound and should be more appropriately formulated as $[NH_4 \cdot (CH_2)_6N_4]BF_4$. The shape complementarity of the BF_4^- guest anions and the cavities of a super-diamond (super-zincblende) host architecture of H-bonded NH_4^+ and urotropin is apparently less good than in the super-wurtzite alternative, and various qualitative speculations may be advanced to explain this; a more rigorous molecular modelling study should provide quantitative insight. The ammonium-

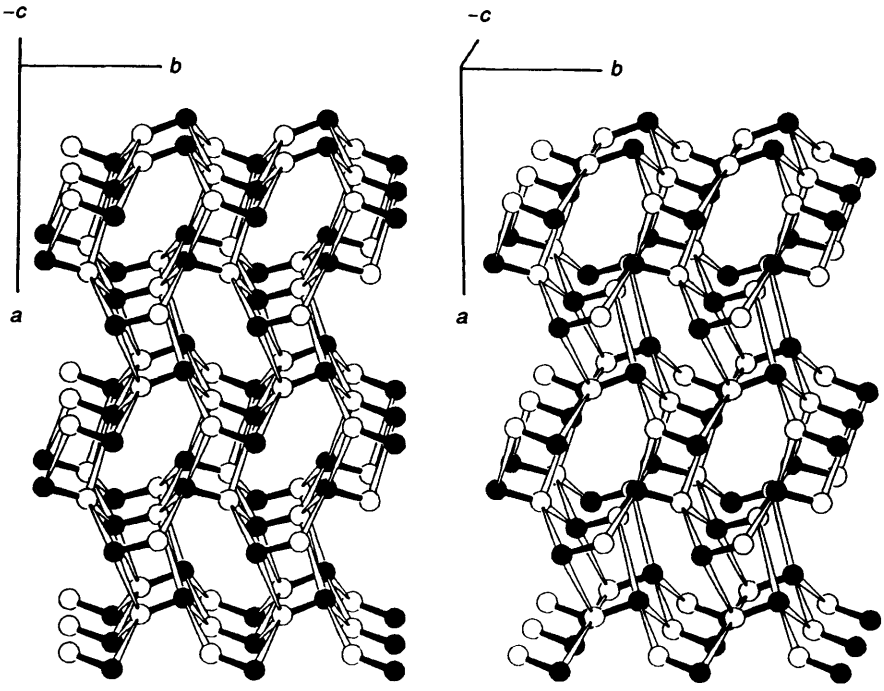

Fig. 13 Stereoview of the super-tetrahedral H-bonded 3D network of crystalline hydroxylamine, $HONH_2$ (based on O, N X-ray coordinates of ref. 32, H atoms not localized in this analysis): O, white, N, black spheres; O(H)N hydrogen bonds drawn as open white, covalent O–N bonds as filled black sticks. The H-bonds span undulating sheets consisting of fused distorted 'super-cyclohexane' boats connected covalently by the O–N bonds neither diamond- nor wurtzite-like (non-equivalent ON distances of the H-bonds, 2.74, 3.07, 3.18 Å [32]).

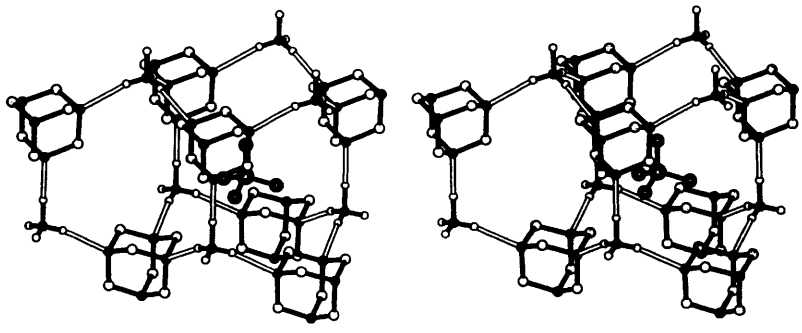

Fig. 14 Stereoview of the combined super-iceane and super-bicyclo[2.2.2]octane building block cut out of the cationic H-bonded, undistorted super-wurtzite network of $[NH_4 \cdot (CH_2)_6N_4]BF_4$ (based on the X-ray coordinates of ref. 33; non-equivalent NN distances of H bonds, 2.999 and 3.025 Å): N, black, C, white large spheres, methylene H atoms omitted; H bonds drawn as open white sticks. The 3D network is made up of H-bonded ammonium cations and urotropin; each of its super-iceane cages enclathrates a tetrafluoroborate anion, which is also illustrated.

urotropin super-wurtzite network involves two symmetry-independent H_3N^+–H···N hydrogen bonds with NN distances of 2.999 and 3.025 Å. For an N(H)N hydrogen bond, these values are comparatively short, most likely chiefly due to the positive ammonium charge. The negative charge on the BF_4^- anions might also help to contract the host lattice and thus the hydrogen bonds. It is amusing to note that the original authors of this interesting super-tetrahedral structure confined their published discussion to essentially the single statement: 'Indications supporting hydrogen bonds are not observed' [33]!

Conclusions

The present study shows that even with standard organic chemicals interesting new supramolecular chemistry can be engineered on the basis of simple but effective complementarity criteria. Specifically, it could be shown that due to the complementarity of the hydroxy and amino groups, molecular recognition occurs among alcohols and primary amines. The respective molecular complex formation is accompanied by a 50% increase of the number of hydrogen bonds, and in the case of the present dialcohols and diamines, as well as amino alcohols, leads to H-bonded three-dimensional, super-tetrahedral networks, in particular super-diamond and super-wurtzite architectures (3D 4-connected nets). However, other network types should also be possible, including sheet-like 2D 4-connected nets. Indeed, the study of H-bonded supramolecular structures may lead to the creation or perception of entirely new network connectivities.

The present concept of H-bond maximization through complex formation between systems with complementary H-bond donors and acceptors may be extended from the three-dimensional tetrahedral to the two-dimensional trigonal-planar case. An example is the pair cyanuric acid–melamine forming a very stable 1 : 1 molecular complex, which probably takes up a planar trigonal 'super-graphite' sheet structure (the analogy with trigonal boron nitride, BN, being even closer) with triply hydrogen-bonded molecular neighbours [Fig. 15(*a*)].[34] It is easily seen that the in-plane H-bond donors and acceptors (lone pairs) of cyanuric acid and melamine are perfectly complementary both as regards their number and directionality: cyanuric acid has three in-plane donors and six acceptors,

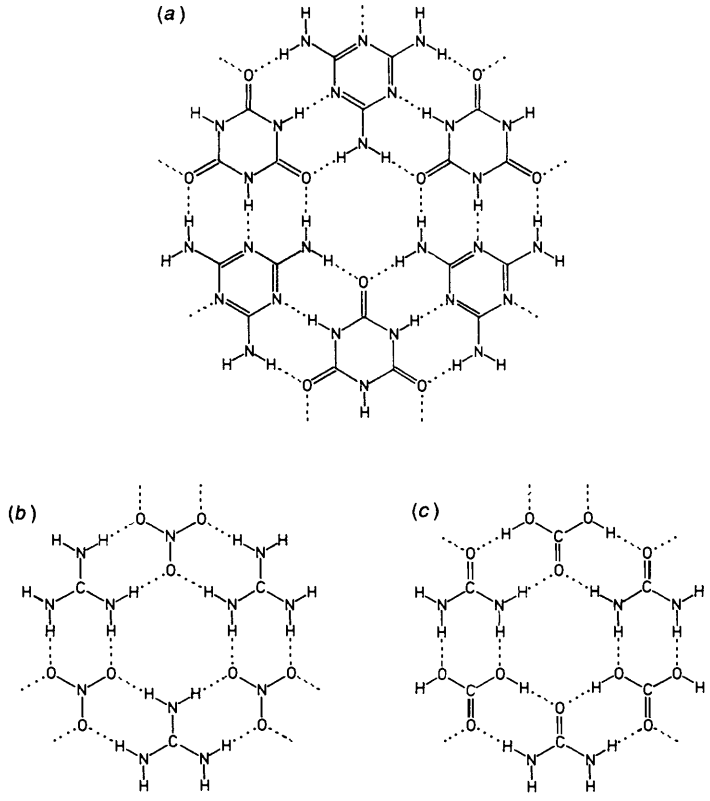

Fig. 15 (*a*) Probable triply H-bonded 2D sheet architecture of the 1 : 1 complex between melamine and cyanuric acid; (*b*) probable doubly H-bonded sheet structure of guanidinium nitrate; (*c*) suggested doubly H-bonded sheet structure of the hypothetical 1 : 1 complex between urea and carbonic acid

melamine six donors and three acceptors. Thus in the 1 : 1 complex the number of donors and acceptors is balanced, which, together with the directional complementarity, allows maximum H-bonding.[35] Another lucid example is provided by guanidinium nitrate, $C(NH_2)_3NO_3$, which is likely to form analogous, yet only doubly H-bonded planar sheets [Fig. 15(*b*)]. In line with this conjecture, we obtained large trigonal-pyramidal crystals of this salt from aqueous solution, which are rather hard along the trigonal axis, yet very soft perpendicular to it (graphite-like behaviour). X-Ray photographs show reflections of poor sharpness probably owing to disturbed, partially disordered sheet stacking. Crude unit-cell dimensions could nevertheless be obtained, which support the suggested sheet structure (rhombohedral crystal symmetry, hexagonal cell edges approximately $a = 7.3$, $c = 18.6$ Å, indicating an O(H)N distance of 2.90 Å and an average stacking separation of $c/6 = 3.1$ Å; the large c constant implies a rather complex stacking pattern with six sheets per repeating unit). This architecture is very similar to that of orthoboric acid, $B(OH)_3$, which displays graphitic cleavage properties, too (potential lubricants). With its trigonally oriented three OH groups and three in-plane lone pairs, boric acid is of course perfectly self-complementary as regards optimal in-plane hydrogen bonding. The structure of guanidinium perchlorate is also of this sheet-type with one oxygen atom not involved in H-bonding.[36] A third hypothetical example worth speculating about in this context concerns a conceivable 1 : 1 complex between urea, $CO(NH_2)_2$, and carbonic acid, $CO(OH)_2$ [Fig. 15(*c*)]. Strictly speaking, only stoichiometric complementarity of in-plane H-bond donors and acceptors is present in this molecular pair without, however, precluding the possibility of creating doubly H-bonded super-graphite trigonal sheets similar to those of guanidinium nitrate or $B(OH)_3$. 'Expanding' carbonic acid in this hypothetical aggregate to 5-nitroisophthalic acid may also be envisaged, but the doubly H-bonded honeycomb sheets of such a complex would suffer from appreciable hexagonal holes.

Two potential applications exploiting the affinity between alcohols and primary amines as established in the present work, might be the following. (1) Alcohol–amine complexes could be useful as crystalline supramolecular derivatives of alcohols and amines with poor crystallization propensity, in particular of polyols, notoriously troublesome in this respect. (2) Bio-ethanol from fermentation processes is obtained in dilute aqueous solution and has to be concentrated for fuel use by energetically costly means. An extractive procedure appears conceivable using cheap liquid (*e.g.*, aromatic) amines immiscible with water. Although interesting, ethanol-complexing molecular agents so far discussed in this context[37] appear too sophisticated and expensive to be of practical use on a technologically large scale. On the other hand, an obvious drawback of amines for ethanol extraction would be their toxicity.

Acknowledgements

Financial support of the *Fonds der Chemischen Industrie* is gratefully acknowledged.

Appendix

Crystal Structure of the 1 : 1 *Molecular Complex Between Hydroquinone and the Double Schiff Base* 1,4-*Bis(isopropylideneamino)benzene* **1•7**.—This complex was inadvertently obtained when attempting to crystallize the hydroquinone–*p*-phenylenediamine complex **1•3** from *hot* acetone solution. Similarly, Schiff-base formation had previously been encountered in the course of early crystallographic work on *p*-aminophenol, and the ensuing confusion was at last resolved by a crystal structure analysis of 4-isopropylideneamino-

phenol[38] showing the molecules to be aggregated in chains through O(H)N hydrogen bonds between the hydroxy oxygen and imino nitrogen atoms (ON distance 2.66 Å). We deemed it worthwhile to look at the crystal structure of **1**·**7** in detail by X-ray methods and briefly report the results in order to add yet another facet to the notoriously rich supramolecular chemistry of hydroquinone.

Crystals of **1**·**7** are monoclinic, a = 5.680(1), b = 11.830(2), c = 12.569(4) Å, β = 99.31(3)°, space group $P2_1/n$ with Z = 2 formula units in the cell, *i.e.*, crystallographic centrosymmetry of both complex components, d_x = 1.189, d_m = 1.20 g cm^{-3}; structure solution and refinement (C, N, O anisotropic, H isotropic) based on 873 reflections with $F_o > 4\sigma(F_o)$, R = 0.069, R_w = 0.061, maximum residual electron density 0.23 e Å^{-3}. Atomic coordinates and temperature factors, and a stereo view of the crystal structure have been deposited at the Cambridge Crystallographic Data Centre. The molecular geometries of **1** and **7** in their complex **1**·**7** are unexceptional besides a slight out-of-plane bending deformation at C(11) and some bond angle widenings in **7**, such that more room is provided for the congested methyl group C(16)H_3.

The crystal structure of the molecular complex **1**·**7** is characterized by zig-zag chains of alternating hydroquinone and double-Schiff-base molecules held together by single O(H)N hydrogen bonds (ON distance 2.758 Å). The aromatic rings in the chains are not co-planar as in quinhydrone[39] (with chains of H-bonded quinone and hydroquinone molecules) due to the non-planarity of the double-Schiff base **7**. For steric reasons, the isopropylidene groups are twisted out of the aromatic plane around the C–N single bonds by 73°. The ensuing loss of π-overlap is partially compensated by overlap of the nitrogen lone pairs with the aromatic π-system, which in turn is weakened, however, by the H-bonding. The respective conformational behaviour of 4-isopropylideneaminophenol as well as its H-bond characteristics[38] are similar. On the whole, it may be stated that the crystal structure and H-bonding relationship between **1**·**7** and 4-isopropylideneaminophenol is a one-dimensional analogue of that between **1**·**3** and **5** (intermolecular *vs.* intramolecular combination of hydroxy and imino, and of hydroxy and amino groups, respectively).

References

1 D. Eilerman and R. Rudman, *Acta Crystallogr., Sect. B*, 1979, **35**, 2458; F. J. Llewellyn, E. G. Cox and T. H. Goodwin, *J. Chem. Soc.*, 1937, 883.

2 H. M. Powell, *J. Chem. Soc.*, 1948, 61; S. V. Lindeman, V. E. Shklover and Yu. T. Struchkov, *Cryst. Struct. Commun.*, 1981, **10**, 1173; D. D. MacNicol, in *Inclusion Compounds*, eds. J. L. Atwood, J. E. D. Davies and D. D. MacNicol, Academic Press, New York, 1984, Vol. 2, p. 1.

3 J.-M. Lehn, *Angew. Chem., Int. Ed. Engl.*, 1988, **27**, 89; 1990, **29**, 1304; D. J. Cram. *Angew. Chem., Int. Ed. Engl.* 1988, **27**, 1009.

4 (*a*) W. C. Hamilton, B. Kamb, S. J. LaPlaca and A. Prakash, *Physics of Ice*, Plenum, New York, 1969, p. 44*ff*; T. C. W. Mak and G.-D. Zhou, *Crystallography in Modern Chemistry*, Wiley, New York, 1992, p. 185*ff*; (*b*) Note that the OH · · · O distance in ice is shorter than in the gas-phase water dimer and in liquid water (1.72, 2.02 and 1.85 Å, respectively); see: G. A Jeffrey and W. Saenger, *Hydrogen Bonding in Biological Structures*, Springer, Berlin, 1991, p. 27. This helps to reduce the size of the holes in ice.

5 A. Kofler, in *Landolt-Börnstein, Zahlenwerte und Funktionen aus Physik, Chemie, Astronomie, Geophysik und Technik*, 6th edn., eds. K. Schäfer and E. Lax, Springer, Berlin, 1956, Vol. II, Part 3, p. 350*ff*.

6 E. A. Moelwyn-Hughes, *Physical Chemistry*, 2nd edn., Pergamon, Oxford, 1961, 1964, p. 1060.

7 S. W. Benson and E. D. Siebert, *J. Am. Chem. Soc.*, 1992, **114**, 4269.

8 (*a*) G. A. Jeffrey, in *Inclusion Compounds*, eds. J. L. Atwood, J. E. D. Davies and D. D. MacNicol, Academic Press, New York, 1984, Vol. 1, p. 135; (*b*) S. Wei, Z. Shi and A. W. Castleman, *J. Chem. Phys.*, 1991, **94**, 3268; X. Yang and A. W. Castleman, *J. Am. Chem. Soc.*, 1989, **111**, 6845.

9 S. Suzuki, P. G. Green, R. E. Bumgarner, S. Dasgupta, W. A. Goddard III and G. A. Blake, *Science*, 1992, **257**, 942.

10 G. Ferguson, J. F. Gallagher, C. Glidewell, J. N. Low and S. N. Scrimgeour, *Acta Crystallogr., Sect. C*, 1992, **48**, 1272.

11 O. Ermer and L. Lindenberg, *Helv. Chim. Acta*, 1991, **74**, 825; O. Ermer, *J. Am. Chem. Soc.*, 1988, **110**, 3747.

12 Relevant work on supramolecular engineering by means of hydrogen bonds: (*a*) K. S. Jeong, T. Tjivikua, A. Muehldorf, G. Deslongchamps, M. Famulok and J. Rebek, *J. Am. Chem. Soc.*, 1991, **113**, 201; J. Rebek, *Angew. Chem., Int. Ed. Engl.*, 1990, **29**, 245; R. Wyler, J. de Mendoza and J. Rebek, *Angew. Chem.*, 1993, **105**, 1820; (*b*) R. P. Dixon, S. J. Geib and A. D. Hamilton, *J. Am. Chem. Soc.*, 1992, **114**, 365; S. J. Geib, C. Vicent, E. Fau and A. D. Hamilton, *Angew. Chem., Int. Ed. Engl.*, 1993, **32**, 119; (*c*) G. M. Whitesides, J. P. Mathias and C. T. Seto, *Science*, 1992, **254**, 1312; J. P. Mathias, E. E. Simanek, C. T. Seto and G. M. Whitesides, *Angew. Chem.*, 1993, **105**, 1848; (*d*) M. C. Etter and S. M. Rentzel, *J. Am. Chem. Soc.*, 1991, **113**, 2586; M. C. Etter, *Acc. Chem. Res.*, 1990, **23**, 120; (*e*) Z. Berkovitch-Yellin, S. Ariel and L. Leiserowitz, *J. Am. Chem. Soc.*, 1983, **105**, 765; L. Leiserowitz and A. T. Hagler, *Proc. R. Soc. London*, 1983, **388**, 133; (*f*) G. R. Desiraju, *Crystal Engineering. The Design of Organic Solids*, Elsevier, Amsterdam, 1989.

13 O. Ermer, *Helv. Chim. Acta*, 1991, **74**, 1339; O. Ermer and C. Röbke, *J. Am. Chem. Soc.*, 1993, **115**, 10077.

14 C. J. Brown, *Acta Crystallogr.*, 1951, **4**, 100.

15 K. Maartmann-Moe, *Acta Crystallogr.*, 1966, **21**, 979; S. C. Wallwork and H. M. Powell, *J. Chem. Soc.*, 1980, 641; F. L. Hirshfeld, *Isr. J. Chem.*, 1964, **2**, 87.

16 A. I. Kitaigorodsky, *Molecular Crystals and Molecules*, Academic Press, New York, 1973; Chap. IA.6.

17 N. W. Larsen, *J. Mol. Struct.*, 1979, **51**, 175.

18 (*a*) Z. P. Poveteva and Z. V. Zvonkova, *Kristallografija*, 1975, **20**, 69; (*b*) M. Colapietro, A. Domenicano, G. Portalone, G. Schultz and I. Hargittai, *J. Phys. Chem.*, 1987, **91**, 1728.

19 D. G. Lister, J. K. Tyler, J. H. Hög and N. W. Larsen, *J. Mol. Struct.*, 1974, **23**, 253.

20 For summaries and relevant references, see: (*a*) A. Almenningen, O. Bastiansen, L. Fernholt, B. N. Cyvin, S. J. Cyvin and S. Samdal, *J. Mol. Struct.*, 1985, **128**, 59; (*b*) H. Calleau, J. L. Bandour and C. M. E. Zeyen, *Acta Crystallogr., Sect. B*, 1979, **35**, 426; (*c*) O. Bastiansen and S. Samdal, *J. Mol. Struct.*, 1985, **128**, 115; (*d*) C. P. Brock and K. L. Haller, *J. Phys. Chem.*, 1984, **88**, 3570; C. P. Brock, M.-S. Kuo and H. A. Levy, *Acta Crystallogr., Sect. B*, 1978, **34**, 981.

21 G. P. Charbonneau and Y. Delugeard, *Acta Crystallogr., Sect. B*, 1977, **33**, 1586; 1976, **32**, 1420.

22 *International Tables for Crystallography*, 2nd edn., ed. T. Hahn, Reidel, Dordrecht, 1987, Vol. A, *Space Group Symmetry*.

23 E. G. Cox, D. W. J. Cruickshank and J. A. S. Smith, *Proc. R. Soc. London, Ser. A*, 1958, **247**, 1; G. E. Bacon, N. A. Curry and S. A. Wilson, *Proc. R. Soc. London, Ser. A*, 1964, **279**, 98; G. A. Jeffrey, J. R. Ruble, R. K. McMullan and J. A. Pople, *Proc. R. Soc. London, Ser. A*, 1987, **414**, 47.

24 J. Trotter, *Acta Crystallogr.*, 1961, **14**, 1135; A. Hargreaves and J. H. Rizvi, *Acta Crystallogr.*, 1962, **15**, 365.

25 For a discussion of edge-to-face and face-to-face interactions among aromatic systems, see: W. L. Jorgensen and D. L. Severance, *J. Am. Chem. Soc.*, 1990, **112**, 4768.

26 T. Kitazawa, S. Nishikiori, R. Kuroda and T. Iwamoto, *Chem. Lett.*, 1988, 1729.

27 B. F. Hoskins and R. Robson, *J. Am. Chem. Soc.*, 1990, **112**, 1546.

28 M. Simard, D. Su and J. D. Wuest, *J. Am. Chem. Soc.*, 1991, **113**, 4696.

29 H. Schäfer, H. G. von Schnering, K.-J. Niehues and H. G. Nieder-Vahrenholz, *J. Less-Common Met.*, 1965, **9**, 95.

30 L. Pauling and P. Pauling, *Proc. Natl. Acad. Sci. USA*, 1968, **60**, 362.

31 D. Mootz, D. Brodalla and M. Wiebcke, *Acta Crystallogr., Sect. C*, 1989, **45**, 754.

32 E. A. Meyers and W. N. Lipscomb, *Acta Crystallogr.*, 1955, **8**, 583; B. Jerslev, *Acta Crystallogr.*, 1958, **11**, 511; J. Donohue, *Acta Crystallogr.*, 1958, **11**, 512.

33 E. Fluck and W. Schwarz, *Z. Anorg. Allg. Chem.*, 1978, **444**, 121.

34 C. T. Seto and G. M. Whitesides, *J. Am. Chem. Soc.*, 1990, **112**, 6409.

35 Similarly, complementary derivatives of 2,4,6-triaminopyrimidine

and barbituric acid have been shown to form 1:1 aggregates with triply H-bonded chain structures: J.-M. Lehn, M. Mascal, A. DeCian and J. Fischer, *J. Chem. Soc., Chem. Commun.*, 1990, 479.
36 Z. Pajak, M. Grottel and A. E. Koziol, *J. Chem. Soc., Perkin Trans. 2*, 1982, **78**, 1529. Interesting crystal engineering of guanidinium sulfonates has been reported recently: V. A. Russell, M. C. Etter and M. D. Ward, *J. Am. Chem. Soc.*, 1994, **116**, 1941.
37 F. Toda, *Top. Curr. Chem.*, 1987, **140**, 43; F. Toda, in *Inclusion Compounds*, eds. J. L. Atwood, J. E. D. Davies and D. D. MacNicol, Oxford University Press, Oxford, 1991; Vol. 4, p. 126*ff*; S. A. Bourne, L. R. Nassimbeni, K. Skobridis and E. Weber, *J. Chem. Soc., Chem. Commun.*, 1991, 282.
38 D. R. Holmes and H. M. Powell, *Acta Crystallogr.*, 1953, **6**, 256.
39 T. Sakurai, *Acta Crystallogr.*, 1965, **19**, 320; *Sect. B*, 1968, **24**, 403.

Paper 3/05750J
Received 23*rd September* 1993
Accepted 1*st February* 1994